

**Studies on chemical characteristics and source
apportionment and Long-range transport of
PM_{2.5} in Niigata, eastern Japan**

Name: Li Ping

Doctoral Program in Environmental Science and Technology

Graduate School of Science and Technology

Niigata University

Contents

ABSTRACT.....	1
1. INTRODUCTION	2
1.1 Fine particulate matter	2
1.2 The research review of $PM_{2.5}$ characterization in Japan	3
1.3 The research significance of $PM_{2.5}$ in Niigata	4
2. MATERIAL AND METHODOLOGY	6
2.1 The monitoring station	6
2.2 Sampling and Chemical analysis	7
2.3 Quality assurance (QA) and Quality control (QC)	9
2.4 PMF and PSCF Analytical Method	12
3. RESULTS AND DISCUSSION.....	15
3.1 Temporal variations of $PM_{2.5}$ mass concentration	15
3.2 Chemical characteristics of $PM_{2.5}$	17
3.2.1 Water soluble ions	17
3.2.2 Carbonaceous species analysis.....	19
3.2.3 Metallic elements analysis	21
3.2.4 Contribution of Chemical components between $PM_{2.5}$ and $PM_{>2.5}$ in ambient air	23
3.3 $PM_{2.5}$ mass balance	25
3.4 Major components of $PM_{2.5}$	27
3.5 Relationship between of $PM_{2.5}$ and meteorological factors	30
3.5.1 $PM_{2.5}$ concentration and meteorological factors	30
3.5.2 Major components of $PM_{2.5}$ and meteorological factors	32
3.6 Correlations of chemical components in $PM_{2.5}$	35
3.7 Source apportionment of $PM_{2.5}$ from PMF analysis	38

3.8 <i>Emission regions of PM_{2.5} major sources by PSCF analysis</i>	43
4. CONCLUSIONS.....	53
ACKNOWLEDGMENTS	55

Figure Captions

Fig. 1. Location of the study monitoring station: Niigata-Maki and the reference sites: Sado-seki, Kameda, and Chiba.

Fig. 2. Seasonal variation of water-soluble ion balance.

Fig. 3. Daily variations of PM_{2.5} concentrations at Niigata-Maki, Kameda and Sado-seki site in Niigata.

Fig. 4. The correlation plots of daily PM_{2.5} mass concentrations at Niigata-Maki, Kameda and Sado-seki.

Fig. 5. Seasonal means of PM_{2.5} mass concentration, rainfall, wind speed and temperature at the Niigata-Maki and the near meteorological station.

Fig. 6. Seasonal means of PM_{2.5} mass concentration, rainfall, wind speed and temperature at Kameido site in urban Tokyo.

Fig. 7. Contribution of chemical components in PM

Fig. 8. Seasonal discrepancy between the PM_{2.5} mass and the sums of the aerosol chemical components at Niigata-Maki.

Fig. 9. (a) Annual average concentrations and (b) Annual average contributions of major components in PM_{2.5} at Niigata-Maki (JFY 2015 and 2016), Kameda (JFY 2013), Chiba (JFY 2015) and the Japan national average (JFY 2013).

Fig. 10. Six factors obtained by using the PMF 5.0 model for each source category at Niigata-Maki: (a) sea salt, (b) biomass combustion, (c) soil dust, (d) secondary aerosol, (e) vehicular traffic, (f) industrial activity.

Fig. 11. The annual mean contribution of each source to the ambient PM_{2.5} at Niigata-Maki.

Fig. 12. Potential source regions by using PSCF analysis: (a) sea salt, (b) biomass combustion, (c) soil dust, (d) secondary aerosol.

Fig. 13. Fire spots of biomass burning activity in spring and autumn in Northeast Asia from JFY 2015 to 2016 (<https://firms.modaps.eosdis.nasa.gov/firemap/>).

Fig. 14. Potential source regions of biomass combustion in autumn by using PSCF analysis at Niigata-Maki.

Fig. 15. Potential source regions of soil dust in winter by using PSCF analysis at Niigata-Maki.

Fig. 16. Location of thermal power plants in Japan, referenced from (Electrical Japan, 2017).

Fig. 17. The back trajectory analysis results in spring at Niigata-Maki site in JFY 2015 and 2016.

Table Captions

Table 1. Seasonal intensive sampling periods from May 2015 to February 2017 at Niigata-Maki.

Table 2. Instrumental parameters for microwave digestion procedure.

Table 3. Analytical recoveries of elements in the NIES CRM No.28 Urban Aerosols.

Table 4. Seasonal mean mass concentrations of PM_{2.5}, water soluble ionic species, OC and EC at Niigata-Maki.

Table 5. Seasonal mean concentrations of metallic elements in PM_{2.5} at Niigata-Maki.

Table 6. Annual mean concentrations of water-soluble ionic species, OC and EC at Niigata-Maki.

Table 7. Relationships between meteorological factors and principal components of PM_{2.5} in Niigata

Table 8. Relationships between meteorological factors and major components of PM_{2.5} in urban Tokyo.

Table 9. Correlation matrix among PM_{2.5}, OC, EC, ionic species and metallic elements in PM_{2.5} at Niigata-Maki.

Table 10. Correlation matrix among metallic elements species in PM_{2.5} at Niigata-Maki.

ABSTRACT

Seasonal intensive sampling was undertaken for two weeks during each of four seasons from May 2015 to February 2017 at Niigata-Maki station in Niigata, eastern Japan. Daily mean concentrations of PM_{2.5} ranged from 4.2 $\mu\text{g m}^{-3}$ to 33.4 $\mu\text{g m}^{-3}$ during the observation period, which were lower than Japanese Environmental Quality Standard for PM_{2.5} (35 $\mu\text{g m}^{-3}$). The higher concentrations of SO₄²⁻, NH₄⁺ and OC were observed in spring and summer, which may result from photochemical activity and secondary OC production. The major chemical components of PM_{2.5} at Niigata-Maki site were SO₄²⁻, NO₃⁻, NH₄⁺, OCM, EC and crustal elements. Compared with data at other urban sites, a lower concentration of EC and NO₃⁻ and higher OC/EC ratio were observed at Niigata-Maki site, which may result from no significant stationary source and low vehicular traffic in the rural site. PM_{2.5} source apportionment was characterized by positive matrix factorization (PMF) analysis, and the results inferred four major sources: sea salt (10.2%), biomass combustion (18.9%), soil dust (13.2%) and secondary aerosol (44.4%). The potential source contribution function (PSCF) analysis suggested that the major sources of secondary aerosol and sea salts were domestic in southwest Japan and the Sea of Japan, whereas the sources of biomass combustion and soil dust in specific seasons were long range transportation from the Northeast Asian continent (NEA). Comparing with previous studies in western Japan, this study showed a large domestic contribution of southwest Japan for secondary aerosol, while a larger contribution of the NEA was observed in the previous studies. Significant contribution of biomass combustion from northeast China in autumn and local area in Niigata and southwest Japan in the other seasons was uniquely observed in this study.

Keywords: Secondary aerosol; Biomass combustion; Northeast Asian continent; PMF; PSCF.

1. INTRODUCTION

1.1 *Fine particulate matter*

Fine particulate matter (PM_{2.5}) is a mixture of solid or liquid particles suspended in the air, which pass through a size-selective inlet with a 50 % efficiency cut-off at 2.5 μm aerodynamic diameter. PM_{2.5} is a very complex mixture, mainly consists of water-soluble ions, carbonaceous species, crustal elements and trace elements (Ho *et al.*, 2011; Manousakas *et al.*, 2013; Cheng *et al.*, 2013), derived from various processes and numerous sources including motor vehicles, power plants, industries, agriculture, biomass burning, forest fires and the secondary pollutants through chemical and photochemical reactions. Water-soluble inorganic ions are mainly from secondary ionic aerosols (NO₃⁻, SO₄²⁻ and NH₄⁺), which can directly affect the acidity of precipitation. There are also many kinds of water-soluble organic aerosols. Especially originated from biomass combustion sources. Organic carbon (OC) originates from both natural and anthropogenic sources and contains some toxic substances, such as PAHs. Element carbon (EC) is directly emitted from primary combustion. The crustal elements (Si, Mg, Ca, Al and Fe) are mainly from soil or construction dust. Heavy metals, such as Ni, Cr, Zn, Mn, and Cu, contribute to the trace elements in PM_{2.5}.

PM_{2.5} is considered as an important environmental pollutant and has adverse effects on human health, including effects on the heart, nervous, and vascular system (Leiva G *et al.*, 2013; Zeller *et al.*, 2006; Chan *et al.*, 2006). It is also well documented in various investigations that particulate matter has influence on human health in Japan (Murakami *et al.*, 2006; Yamazaki *et al.*, 2007). Moreover, PM_{2.5} is proved to be linked to degradation of visual range, with the features of light extinction (Yang *et al.*, 2007). To evaluate these effects, components of PM_{2.5} need to be investigated at different temporal and spatial scales because chemical properties in PM_{2.5} are important factors to determine the effects.

1.2 The research review of PM_{2.5} characterization in Japan

Previous studies have investigated chemical components and their variations of PM_{2.5} in Japan, and the long-range transport from East Asia countries. For some examples, secondary and carbonaceous aerosols are associated mostly with PM_{2.5} while the Cl⁻, Na⁺, Ca²⁺ and Mg²⁺ are dominated to the coarse particulate matter in PM_{2.5-10} and PM_{>10} in Yokohama, a megacity in Tokyo metropolitan area (Khan *et al.*, 2010). SO₄²⁻, NO₃⁻, NH₄⁺, OC and EC are the major chemical components in Chiba prefecture, located in Tokyo metropolitan area of Japan, and seasonal fluctuations of EC and OC show that autumn and winter concentrations are relatively higher than those recorded in spring and summer time, this result could be attributed to the impact of burning biomass (Ichikawa *et al.*, 2015). The ratios of Cd/Pb and Pb/Zn in PM_{2.5} in the northern Kyushu area of Japan were close to the aerosol composition in Beijing, which implies the same components of PM_{2.5} was transported from the NEA to the western Japan. (Kaneyasu *et al.*, 2014). High levels of PAHs in total suspended particles (TSP) are transported from the NEA to western Japan (Coulibaly *et al.*, 2015). Moreover, observation studies, sensitivity analysis by using a regional chemical transport model demonstrated that contribution from central north China accounts for 50–60% of PM_{2.5} at a remote island in western Japan except in summer (Ikeda *et al.*, 2014). In addition to modelling researches. some studies for Source-Receptor analysis of PM_{2.5}. Positive matrix factorization (PMF) and chemical mass balance (CMB) were demonstrated for synthetic datasets that suppose ambient organic aerosol mass spectra from diesel exhaust particles as a primary organic aerosol (POA) and m-xylene-derived secondary organic aerosol (SOA) (Hiroyuki Hagino, 2017). Trans-boundary transport of PM_{2.5} to the Western Japan and Japan Sea side regions based on the Source-Receptor analysis, and the modeled source-receptor ratio in Fukuoka and the observed PM_{2.5} concentration decrease in Beijing-Tianjin-Shandong area explained the recent decreasing trend of PM_{2.5} (13% decrease from 2014 to 2016) at Fukuoka (Itsushi *et al.*, 2017).

1.3 The research significance of PM_{2.5} in Niigata

Niigata City is the capital and the most populous city of Niigata Prefecture located in eastern Japan. It lies on the coast of the Sea of Japan and faces the Northeast Asian continent, and the climate is strongly affected by the circulation of the East Asian Monsoon over East Asia, covering eastern China, the Korean Peninsula and Japan. In winter it's dominated by cold currents from the northwest, while in summer the wet and humid currents of tropical origin prevail. Some studies reported that the effects of long-range transport on the areas located downstream of large emission sources play a major role in ambient air quality (Shimadera *et al.*, 2009). Since the NEA is upwind with respect to Niigata during the winter monsoon period, PM_{2.5} in Niigata is probably influenced by long-range transport from the NEA. However, few observation studies have focused on fine particles across the coast of the Sea of Japan from the NEA, such as transboundary transport of anthropogenic sulfur in PM_{2.5} (Inomata *et al.*, 2016), long-range transport from the NEA of biomass combustion (Huo *et al.*, 2016), and long term variations of PAHs in total suspended particles at a background site on Noto Peninsula (Tang *et al.*, 2015). Therefore, it is important to identify the sources of PM_{2.5} in a coastal city of the Sea of Japan, such as Niigata, and contribution to long-range transportation from the NEA in order to provide scientific findings for evaluation of atmospheric impact of PM_{2.5} in eastern Japan.

In this research, a field observation study including seasonal intensive measurement of PM_{2.5} was conducted from May 2015 to February 2017 at the Niigata-Maki national acid deposition monitoring station in Niigata, eastern Japan. A comprehensive analysis of thirty three chemical components (including EC, OC, Cl⁻, NO₃⁻, SO₄²⁻, Na⁺, NH₄⁺, K⁺, Mg²⁺, Ca²⁺ and 23 metallic elements) in PM_{2.5} was implemented and the seasonal variations of chemical characteristics in PM_{2.5} were elucidated. Then, statistical analyses of correlation matrix, positive matrix factorization (PMF) for annual and potential source contribution function (PSCF) for annual and specific season were conducted in order to identify major sources of PM_{2.5} in Niigata, and also

identify the long-range transport from the NEA.

2. MATERIAL AND METHODOLOGY

2.1 *The monitoring station*

Niigata-Maki national acid deposition monitoring station (37°48'33", 138°51'09", 52 m altitude) is located at the foot of Mt. Kakuda (482 m a.s.l.), 1 km from the seashore, and 25 km southwest of the center in Niigata city, the capital of Niigata prefecture, Japan, as shown in Fig. 1. This station is constructed by the Ministry of Environment, Japan to monitor acid deposition and air pollutant concentration to investigate acid deposition in rural area on the coast of the Sea of Japan. There is no industrial source near Niigata-Maki site but a small community (approximately 1300 population) was located in 2 km the northwest of the station, and thus it is classified as a rural station. Air masses reaching the station are dependent on seasonal wind patterns, which is affected by the monsoon circulation: in winter the northwest cold currents will prevail, while in summer they will be replaced by the hot and humid currents of Pacific Ocean. Therefore, the Niigata-Maki site is suitably located to observe the long-range transport of air pollutants.

For the reference data, I used PM_{2.5} data at the Sado-seki national acid deposition monitoring station (38°14'59", 138°24'00"), which is classified as a remote station and the Kameda air quality monitoring station (37°87'26", 139°10'17"), which is classified as a urban station. The data of Kameda and Sado-seki sites are cited from the Web site of the Ministry of the Environment, Japan (MOEJ) (MOEJ, 2016). Furthermore, I also used the PM_{2.5} continuous monitoring data at the Chiba and Kameido sites are located in Tokyo Metropolitan Region of eastern Japan and classified as an urban station. Chiba site was conducted as a full year continuous monitoring of PM_{2.5} by a research project. (Ichikawa *et al.*, 2015), and Kameido site (35°69'93", 139°82'51") is cited from the Web site of MOEJ.



Fig. 1. Location of the study monitoring station: Niigata-Maki and the reference sites: Sado-seki, Kameda and Tokyo metropolitan sites.

2.2 Sampling and Chemical analysis

Daily PM_{2.5} samples were taken for two weeks during each of four seasons from May 2015 to February 2017, and the daily sampling time was conducted from noon to noon in the next day. We collected a total of 106 daily samples during two years, as shown in Table 1. PM_{2.5} samples were collected on the PTFE membrane filters (Zefluor, 47 mm in diameter and 2.0 μm in pore size, Pall Co., USA) using a low volume sampler (Model 2025, Thermo Fisher Scientific, Inc., USA), designed that a flow rate is 16.7 L min⁻¹ and sequentially 24-hour sampling for 14 days. The PTFE filters were used for mass concentration, water-soluble ions and metallic elements measurement. PM_{2.5} samples were also collected on the quartz filters (2500QAT-UP, 8×10 inches, Pall Co., USA) by using a high volume sampler (HV-1000F, Sibata Scientific Technology Ltd., Japan) and PM_{2.5} impactor (HVI-2.5, Tokyo Dylec Co., Japan), designed that a flow rate is 576 L min⁻¹. By using this sampler, PM_{2.5} was sampled continuously for the first 3 days of each period. After that, the daily sampling was conducted for the middle 7 days, and then continuous sampling was conducted for the last 4 days of each period. We used the average concentration for daily data in continuous sampling period. The quartz filters were used for carbonaceous species measurement. The two samplers were set at 5 meters above the ground and 1.5 m above the rooftop.

Table 1. Seasonal intensive sampling periods from May 2015 to February 2017 at Niigata-Maki.

Sampling Year	Spring	Summer	Autumn	Winter
JFY 2015	2015.05.08 - 2015.05.20	2015.07.22 - 2015.08.04	2015.10.21 - 2015.11.03	2016.01.20 - 2016.02.02
JFY 2016	2016.05.09 - 2016.05.17	2016.07.21 - 2016.08.03	2016.10.21 - 2016.11.03	2017.01.19 - 2017.02.02

*JFY denotes the Japanese fiscal year: JFY 2015 and JFY 2016 is the period from April 2015 to March 2016 and April 2016 to March 2017, respectively.

The mass concentrations of sample filters were determined gravimetrically by using the electronic microbalance (MSE2.7S-000, sensitivity = 0.1 μg , Sartorius AG, Germany) under controlled temperature (20–23°C) and relative humidity (RH at 35–45%). Teflon filters were stored under controlled conditions of temperature and relative humidity for at least 24 hours before and after sampling, and then passed through a static electricity remover before being weighed at least twice, and the acceptance difference between two readings was 3 μg , all processes were performed in weighing chamber (PWS-PM2.5, Dylec Co., Japan).

For analyses of water-soluble ion, A half of a filter was extracted with 20 mL of Milli-Q water (18.2 $\text{M}\Omega \cdot \text{cm}$) for 30 minutes by using a shaker (SR-2w, Taitec Co., Japan). The extracted solution was filtered through a pre-washed membrane filter (A045A025A, 25 mm in diameter and 0.45 μm pore size, Advantec Toyo Co., Japan), and stored in a refrigerator at 4 °C until chemical analysis. Three anions (Cl^- , NO_3^- and SO_4^{2-}) and five cations (Na^+ , NH_4^+ , K^+ , Mg^{2+} and Ca^{2+}) were determined by ion chromatography (ICS-2100 and ICS-1100, Thermo Fisher Scientific, Inc., USA).

Organic carbon (OC) and elemental carbon (EC) were analyzed by using a Desert Research Institute (DRI, USA) Model 2001A thermal/optical carbon analyzer. Collected quartz filters were punched into 0.505 cm^2 pieces to determine OC and EC by the IMPROVE method with the thermal optical reflection protocol (Chow *et al.*, 2001). Depending on combustion temperature and matrix gas, carbonaceous components were fractionated into Organic carbon (OC1 to OC4) and Elemental carbon (EC1 to EC3), and the optical pyrolysis correction of OC (PyC) by

reflectance of helium-neon laser. OC was defined as OC1+OC2+OC3+OC4+PyC and EC was as EC1+EC2+EC3-PyC.

The concentrations of 23 metallic elements (Al, Fe, Ni, Cr, Zn, Mn, Co, Cu, V, Ga, As, Se, Rb, Sr, Sc, Mo, Cd, Sb, Cs, Ba, Pb, Ag and Hg) were analyzed using an Thermo Fisher XSeries 2 Inductively Coupled Plasma Mass Spectrometry (ICP-MS). A quarter of a PTFE filter was put into a PTFE pressure digestion container, and then dissolved in 6 mL of 70% nitric acid (HNO₃) and 3 mL of 50% hydrofluoric acid (HF) and 1mL of 30% hydrogen peroxide (H₂O₂). All digestions were performed in a microwave oven (Ethos 900, Milestone General Inc., USA), the steps of the digestion procedure are shown as Table 2. After the microwave digestion procedure, the digestion containers were heated until the solution volume is reduced to approximately 0.1 mL so that all of HF is evaporated. Then, the samples were diluted with 1 mol L⁻¹ HNO₃ to make a 15 mL solution, and 100 μmol L⁻¹ of internal standard solution (Yttrium) was added into both sample and standard solutions. All reagents used for the digestion procedure were ultra-pure grade quality or better, and all reagent solutions were prepared using MILLI-Q water. All samples and standards were stored in metal-free centrifuge tubes and kept in a refrigerator at 4 °C before analysis.

Table 2. Instrumental parameters for microwave digestion procedure.

step	Time (min.)	Power (w)
1	2	250
2	3	0
3	5	250
4	5	400
5	10	500
6	20	400

2.3 Quality assurance (QA) and Quality control (QC)

The detection limits were calculated as equivalent air concentrations of 3 times of the standard deviations for 8 laboratory blank samples. The detection limits of OC and EC were 0.26

and $0.08 \mu\text{g m}^{-3}$, respectively. The detection limits of Na^+ , NH_4^+ , K^+ , Mg^{2+} , Ca^{2+} , Cl^- , NO_3^- and SO_4^{2-} were 0.02, 0.01, 0.01, 0.01, 0.01, 0.02, 0.03 and $0.03 \mu\text{g m}^{-3}$, respectively. The detection limits of Al, Fe, Ni, Cr, Zn, Mn, Co, Cu, V, Ga, As, Se, Rb, Sr, Sc, Mo, Cd, Sb, Cs, Ba, Pb, Ag and Hg were 22.2, 8.56, 0.03, 1.65, 1.26, 25.7, 1.88, 0.91, 1.83, 14.5, 0.09, 0.36, 0.31, 0.10, 0.53, 0.39, 0.78, 0.13, 0.24, 0.02, 2.02, 0.63 and 0.24 ng m^{-3} , respectively. When the measured concentrations are under these detection limits, we evaluated those as not detected (N.D.).

Working standard samples and ion balance were tested for the water-soluble ion analysis by ion chromatography. The original working standard solution of artificial rain water containing 3 anions of Cl^- , NO_3^- and SO_4^{2-} and 5 cations of Na^+ , NH_4^+ , K^+ , Mg^{2+} and Ca^{2+} was obtained by 18th inter-laboratory comparison project on wet deposition in Acid Deposition Monitoring Network in East Asia (EANET) (Network Center for EANET, 2016). Working standard solutions were prepared from the original solution by diluting 100 times with MILLI-Q water. The accuracy of water-soluble ion analysis was checked by agreement between the measured values and the prepared values within 15% differences.

We also use ion balance for $\text{PM}_{2.5}$ component to check validity of analytical procedure for water-soluble ions. The principle of electroneutrality in an extract of $\text{PM}_{2.5}$ sample requires that the total anion equivalents equal to the total cation equivalents. According to this principle, ion balance in the extract was checked by the below equation.

$$R = (C - A)/(C + A) \times 100 (\%) \quad (1)$$

Where C and A represents total anion and total cation equivalents ($\mu\text{eq L}^{-1}$), and R represents ion balance, respectively. The seasonal variations of water-soluble ion balance were shown in Fig. 2, and all seasonal ion balance values were satisfied with the required criteria (Network Center for EANET, 2010).

To check validity of analytical protocol for metallic elements, the Certified Reference Material (CRM) No. 28 Urban Aerosols were used (National Institute for Environmental Studies, 2015). The recoveries of metallic elements were determined by 9 CRM samples, only the

recoveries of Sb (75%) less than 80%, and the other elements ranged from 83 to 109%. Therefore, Sb concentration was determined by the recovery ratio, as shown in Table 3.

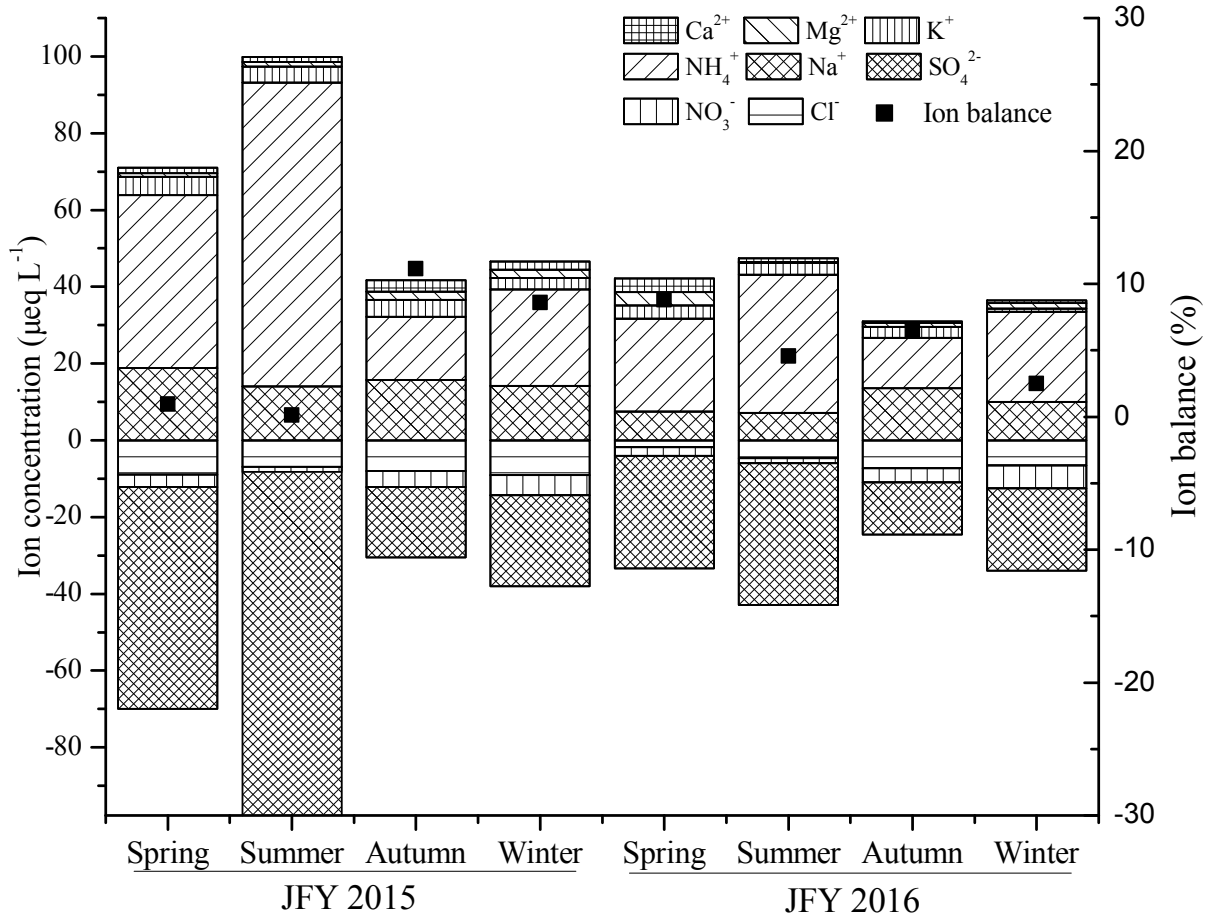


Fig. 2. Seasonal variation of water-soluble ion balance.

Table 3. Analytical recoveries of metallic elements in the NIES CRM No.28 Urban Aerosols.

Metallic elements	Unit	Measured Values	Certified or Reference values	Recovery (%)
Al	%	5.13% ±0.30	5.04% ±0.10 ^a	101.8 ±6.0
Fe	%	2.77% ±0.30	2.92% ±0.17 ^a	94.9 ±10.3
Ni	mg kg ⁻¹	66.9 ±6.0	63.8 ±3.4 ^a	104.9 ±9.4
Cr	mg/kg	64.5 ±6.0	65.6 ^b	98.3 ±9.1
Zn	%	0.12% ±0.01	0.11% ±0.010 ^a	109.1 ±9.1
Mn	mg kg ⁻¹	678.0 ±40	686 ±42 ^b	98.8 ±5.8
Co	mg kg ⁻¹	20.7 ±2.0	22 ^b	94.1 ±9.1
Cu	mg kg ⁻¹	112.9 ±10.0	104 ±12 ^a	108.6 ±9.6
V	mg kg ⁻¹	72.0 ±6.0	73.2 ±7.0 ^a	98.4 ±8.2
As	mg kg ⁻¹	89.4 ±6.0	90.2 ±10.7 ^a	99.1 ±6.7
Se	mg kg ⁻¹	14.3 ±0.7	14.4 ^b	99.3 ±4.9
Rb	mg kg ⁻¹	56.7 ± 2.0	64.1 ^b	88.5 ±3.1
Sr	mg kg ⁻¹	449.5 ±14.0	469 ±16 ^a	95.8 ±3.0
Sc	mg kg ⁻¹	10.2 ±0.6	10.7 ^b	95.3 ±5.6
Mo	mg kg ⁻¹	25.8 ± 1.0	28.4 ^b	90.8 ±3.5
Cd	mg kg ⁻¹	5.0 ±0.1	5.6 ±0.43 ^a	89.3 ±0.9
Sb	mg kg ⁻¹	15.0 ±0.4	20.1 ^b	74.6 ±2.0
Ba	mg kg ⁻¹	722.7 ±16.0	874 ±65 ^a	82.7 ±1.8
Pb	mg kg ⁻¹	357.6 ±25.0	403±32 ^a	88.7 ±7.1

^a, Certified values, ^b, Reference value.

2.4 PMF and PSCF Analytical Method

2.4.1 Positive Matrix Factorization

PMF is a convenient and helpful factor analysis model that decomposes a matrix of sample data into two matrices: factor contribution matrix and factor profile matrix, in terms of observations at the sampling sites (Paatero and Tapper, 1994). The principle can be expressed as:

$$x_{ij} = \sum_{k=1}^p g_{ik} f_{kj} + e_{ij} \quad (2)$$

where x_{ij} is the species concentration of j^{th} in the i^{th} sample, g_{ik} is the contribution of the k^{th} factor

to the i^{th} sample, f_{kj} is the j^{th} species fraction from the k^{th} source, e_{ij} is the residual related with the j^{th} species concentration measured in the i^{th} sample, and p is the total number of independent sources. The object function Q can be allowed to review the distribution of each species in order to evaluate the stability of the solution, which is defined as:

$$Q = \sum_{i=1}^n \sum_{j=1}^m \left[\frac{x_{ij} - \sum_{k=1}^p g_{ik} f_{kj}}{u_{ij}} \right]^2 \quad (3)$$

where u_{ij} is the uncertainty of j^{th} species in the i^{th} sample, which is applied to weight the observations that contain sampling errors, detection limits, missing data and outliers. EPA PMF 5.0 was used to identify the potential sources of $\text{PM}_{2.5}$.

2.4.2 Potential Source Contribution Function

Air parcel back trajectories from the receptor site are represented by the segment endpoints. To calculate the Potential Source Contribution Function (PSCF), the whole geographic region covered by the trajectories is divided into an array of grid cells whose size is dependent on the geographical scale of the problem. The PSCF will be a function of location as defined by the cell indices i and j while the number of segments with endpoints that fall in the ij^{th} cell is denoted by n_{ij} . The number of endpoints in the ij^{th} cell associated with a trajectory that arrives at the sampling site at the same time as a corresponding measured pollutant concentration higher than an arbitrary criterion value is defined by m_{ij} . The PSCF value for the ij^{th} cell is then

$$PSCF_{ij} = m_{ij} / n_{ij}. \quad (4)$$

The PSCF value can be interpreted as the conditional probability that the concentrations of a given pollutant sample greater than the criterion level are related to the passage of air parcels through the ij^{th} cell during transport to the receptor site. That is, cells with high PSCF values are associated with the arrival of air parcels at the receptor site that have measured concentrations higher than the criterion value. These cells are indicative of areas of ‘high potential’ contributions for that pollutant (Wang et al., 2009). The weight function is described as follows:

$$WPSCF_{ij} = \frac{m_{ij}}{n_{ij}} * W(n_{ij}) \quad (5)$$

$$W(n_{ij}) = \begin{cases} 1.00, & 75 < n_{ij} \\ 0.70, & 25 < n_{ij} \leq 75 \\ 0.40, & 8 < n_{ij} \leq 25 \\ 0.20, & n_{ij} \leq 8 \end{cases}$$

We performed a PSCF analysis to identify the preferred atmospheric transport pathways from sources to receptors by TrajStat 1.4.4: GIS-based software that uses various trajectory statistical analysis methods to identify potential sources from long-term air pollution measurement data. This result led us to use PSCF (described below) to estimate the back trajectories at arrival heights of 500, 1000, and 1500 m. Three-day back trajectories at 2-h intervals were computed for arrival heights of 500, 1000, and 1500 m for each of the 106 daily mean samples. The studying field is from 30 to 50 °N, and 120 to 150 °E, which includes more than 95% of area covered by all the paths. Regions with PSCF values ranging from 0.5 to 1 were designated as probable source regions for each factor during the study period.

3. RESULTS AND DISCUSSION

3.1 Temporal variations of PM_{2.5} mass concentration

Table 4 shows that the annual mean mass concentrations of PM_{2.5} were 12.3 $\mu\text{g m}^{-3}$ in JFY 2015 and 9.3 $\mu\text{g m}^{-3}$ in JFY 2016, respectively. Although the monitoring was not conducted for a full year, these values were lower than the annual average of the Japanese Environmental Quality Standard (JEQS) for PM_{2.5} (15 $\mu\text{g m}^{-3}$). Daily mean concentrations of PM_{2.5} ranged from 4.2 $\mu\text{g m}^{-3}$ to 33.4 $\mu\text{g m}^{-3}$ from May 2015 to February 2017, which were lower than the daily average of the JEQS for PM_{2.5} (35 $\mu\text{g m}^{-3}$), as shown in Fig. 3. Daily PM_{2.5} mass concentrations at Niigata-Maki, Kameda and Sado-seki showed similar temporal trends throughout the observation period. The higher mass concentration days were observed in spring and summer, and the lower mass concentration days were observed in autumn and winter (Fig. 3). The seasonal means are discussed in the following paragraph. Daily PM_{2.5} mass concentrations at Niigata-Maki strongly correlated with those at Kameda ($r = 0.82$, $p < 0.01$) and Sado-seki ($r = 0.80$, $p < 0.01$), which implies these sites are probably affected by similar sources or local meteorology (Fig. 4).

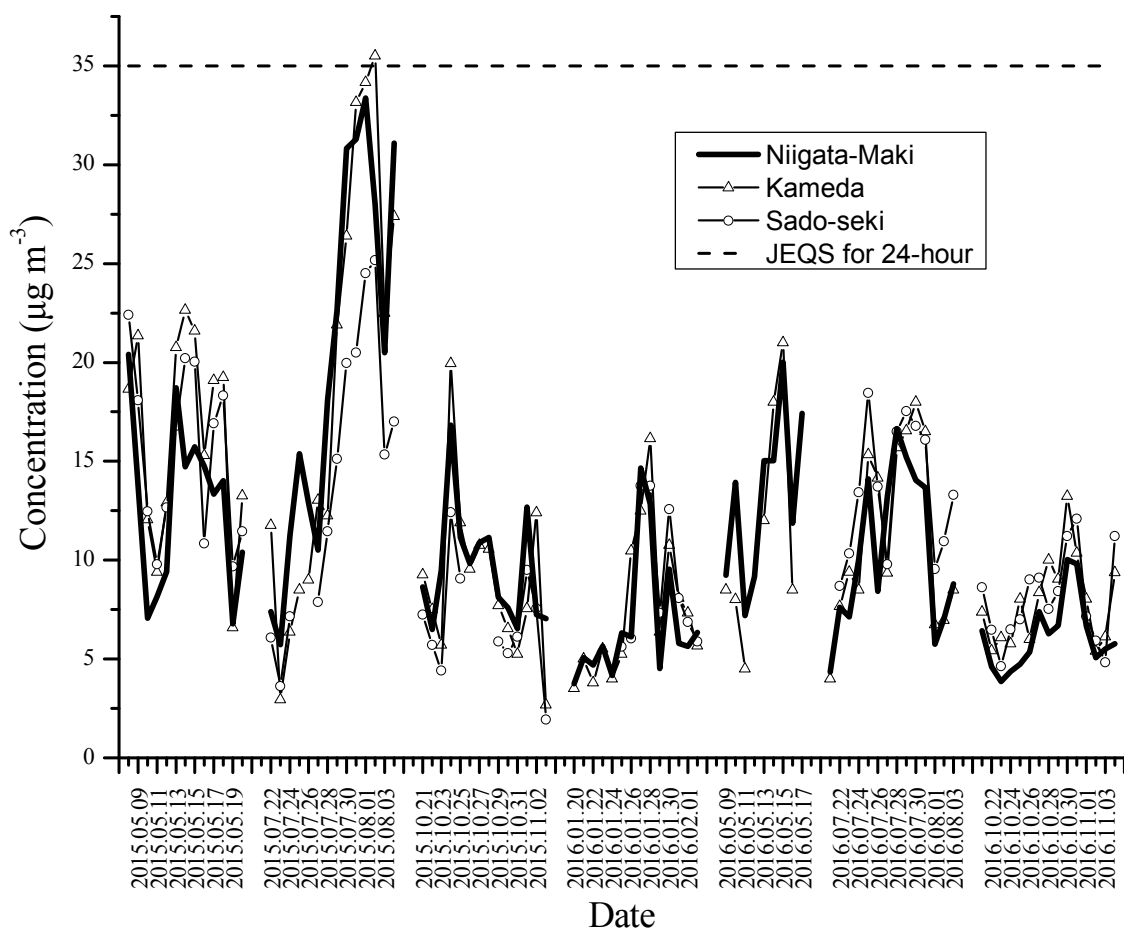


Fig. 3. Daily variations of $\text{PM}_{2.5}$ concentrations at Niigata-Maki, Kameda and Sado-seki site in Niigata.

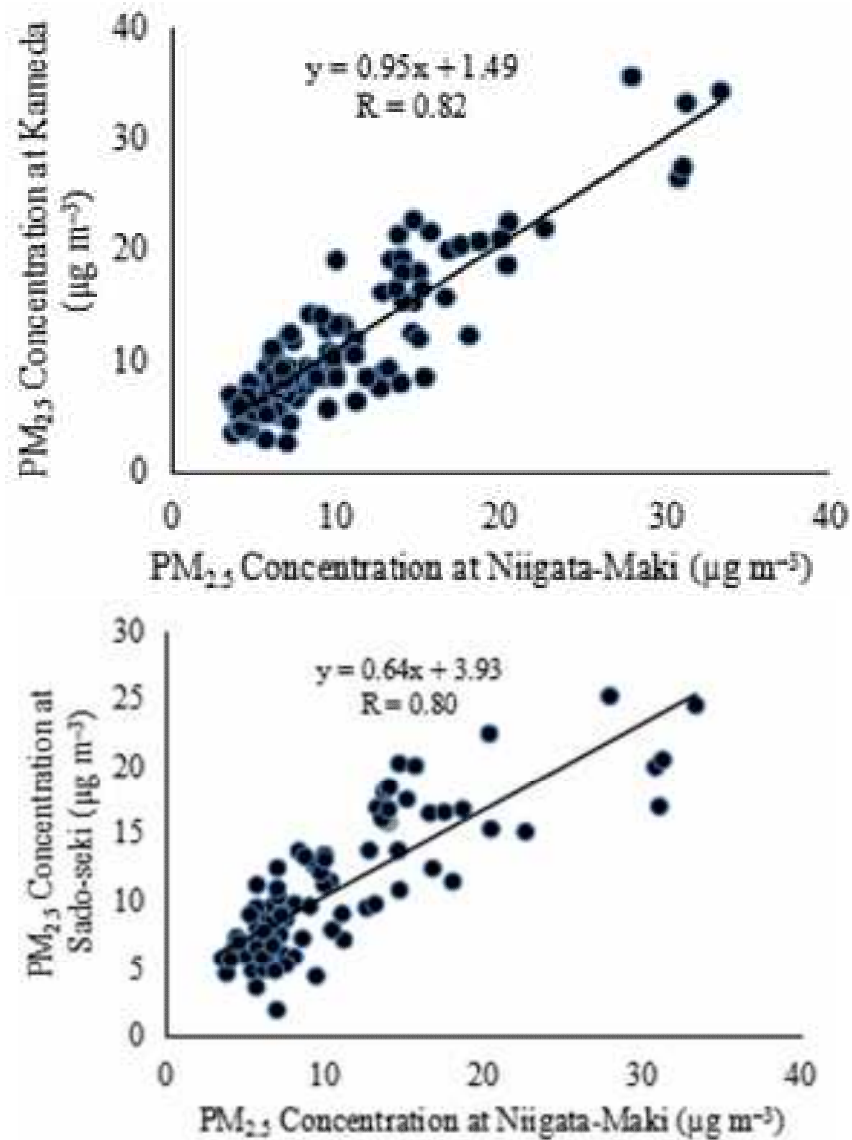


Fig. 4. The correlation plots of daily PM_{2.5} mass concentrations at Niigata-Maki, Kameda and Sado-seki.

3.2 Chemical characteristics of PM_{2.5}

3.2.1 Water soluble ions

Since the sampling site is located close to the seashore, it is important to identify the contributions of water-soluble ions in PM_{2.5} from non-marine and marine sources. Non-sea-salt ion concentration (nss-*M*) was estimated by the following equation assuming that Na⁺ in

particulate matter is solely originated from sea salts:

$$C_{\text{nss}-M} = C_M - KC_{\text{Na}^+} \quad (6)$$

Where M is the target ion, K is the mass ratio of the target ion to Na^+ in seawater ($\text{Mg}^{2+} = 0.1190$, $\text{Ca}^{2+} = 0.0382$, $\text{K}^+ = 0.0370$, $\text{SO}_4^{2-} = 0.2515$, $\text{Cl}^- = 1.79$) (Kennish *et al.*, 1994). The mean contributions of nss-SO_4^{2-} , nss-K^+ , nss-Ca^{2+} , nss-Mg^{2+} and nss-Cl^- to respect ionic concentrations in $\text{PM}_{2.5}$ were 97%, 94%, 34%, 14%, 2%, respectively. This result suggested that the major sources of SO_4^{2-} and K^+ in $\text{PM}_{2.5}$ were non-marine sources, and Cl^- , Mg^{2+} and Ca^{2+} were mainly originated from sea salts.

As shown in Table 4, the annual average concentrations of total water-soluble ions (TWSIs) in JFY 2015 and JFY 2016 were $6.5 \mu\text{g m}^{-3}$ and $3.8 \mu\text{g m}^{-3}$, which accounted for 52.8% and 40.9% of $\text{PM}_{2.5}$ mass concentration in JFY 2015 and JFY 2016, respectively. Clear seasonal variations of TWSIs were observed at Niigata-Maki from May 2015 to February 2017. The seasonal mean concentrations of TWSIs were in the order of summer > spring > winter > autumn (Table 4). The concentrations of sulfate (SO_4^{2-}) and ammonium (NH_4^+) were highest among all water soluble ions in $\text{PM}_{2.5}$. The annual means of SO_4^{2-} and NH_4^+ were 58.0% and 18.5% of the concentration of TWSIs in JFY 2015, 53.1% and 18.6% in JFY 2016, respectively. The higher concentrations of SO_4^{2-} and NH_4^+ were observed in spring and summer. NH_4^+ and SO_4^{2-} are known as tracer species of secondary aerosol, and the increased photochemical activity was one of the possible reasons for enhanced sulfate concentration during the period (Husain *et al.*, 1990). Additionally, the annual mean molar ratio of NH_4^+ to SO_4^{2-} was 1.7 and 1.9 in JFY 2015 and 2016, respectively, the values were close to the molar ratio of NH_4^+ to SO_4^{2-} in $(\text{NH}_4)_2\text{SO}_4$ (2.0). This indicated that NH_4^+ and SO_4^{2-} were mainly from secondary aerosol $(\text{NH}_4)_2\text{SO}_4$.

Table 4. Seasonal mean mass concentrations of PM_{2.5}, water soluble ionic species, OC and EC at Niigata-Maki.

Season	PM _{2.5}	Cl ⁻	NO ₃ ⁻	SO ₄ ²⁻	Na ⁺	NH ₄ ⁺	K ⁺
	μg m ⁻³	μg m ⁻³	μg m ⁻³	μg m ⁻³	μg m ⁻³	μg m ⁻³	μg m ⁻³
Spring	12.9±4.3	0.35±0.32	0.32±0.31	4.61±2.48	0.59±0.41	1.31±0.59	0.24±0.13
JFY Summer	19.9±9.7	0.32±0.29	0.14±0.12	7.34±5.14	0.47±0.28	2.37±1.69	0.23±0.13
2015 Autumn	9.6±3.1	0.38±0.27	0.43±0.11	1.46±0.76	0.54±0.32	0.47±0.22	0.25±0.09
Winter	6.8±3.4	0.45±0.19	0.55±0.50	1.88±0.98	0.48±0.18	0.74±0.52	0.16±0.08
Annual mean	12.3±7.5	0.37±0.27	0.36±0.32	3.81±3.73	0.52±0.28	1.22±1.17	0.22±0.11
Spring	13.2±4.9	0.07±0.19	0.22±0.12	2.34±0.93	0.22±0.19	0.71±0.35	0.19±0.06
JFY Summer	10.4±3.9	0.18±0.18	0.13±0.11	2.94±1.41	0.21±0.20	1.06±0.50	0.17±0.15
2016 Autumn	6.2±1.8	0.38±0.19	0.37±0.17	1.05±0.27	0.49±0.24	0.36±0.12	0.16±0.07
Winter	7.3±3.6	0.30±0.29	0.61±0.49	1.70±1.13	0.31±0.25	0.69±0.53	0.03±0.07
Annual mean	9.3±4.2	0.25±0.24	0.34±0.32	2.01±1.08	0.32±0.24	0.70±0.48	0.14±0.11
Season	Mg ²⁺	Ca ²⁺	TWSIs	EC	OC	OC/EC	
	μg m ⁻³	μg m ⁻³	μg m ⁻³	μgC m ⁻³	μgC m ⁻³		
Spring	0.01±0.03	0.01±0.02	7.4	0.74±0.12	2.58±1.01	3.48	
JFY Summer	0.02±0.01	0.03±0.02	10.8	0.86±0.36	2.14±0.76	2.50	
2015 Autumn	0.04±0.03	0.08±0.03	3.6	0.61±0.26	1.91±1.02	3.12	
Winter	0.04±0.02	0.05±0.02	4.3	0.44±0.38	0.50±0.28	1.12	
Annual mean	0.03±0.02	0.04±0.02	6.5	0.66±0.28	1.78±0.76	2.55	
Spring	0.07±0.01	0.10±0.03	3.9	0.50±0.23	2.34±1.30	4.92	
JFY Summer	N.D.	0.02±0.03	4.7	0.63±0.31	2.09±0.78	3.34	
2016 Autumn	0.02±0.01	N.D.	2.9	0.49±0.88	1.20±1.02	2.24	
Winter	0.02±0.02	0.01±0.02	3.6	0.32±0.22	0.79±0.52	2.45	
Annual mean	0.03±0.01	0.03±0.02	3.8	0.49±0.41	1.61±0.90	3.24	

The values after “±” denote standard deviations based on daily mean concentrations.

TWSIs (Total water-soluble ions) is the summation of Cl⁻, NO₃⁻, SO₄²⁻, Na⁺, NH₄⁺, K⁺, Mg²⁺ and Ca²⁺.

3.2.2 Carbonaceous species analysis

Carbonaceous species in the atmosphere exist in three forms: organic carbon (OC), elemental carbon (EC), and carbonate carbon (CC). Because the ion balance of extract of PM_{2.5} was satisfied with the required criteria, the contribution of carbonate to PM_{2.5} was estimated to less than 5%. Therefore, total carbon (TC) in PM_{2.5} was considered to be the sum of measured OC and EC (μgC) without pre-treatment of removal of carbonate.

As shown in Table 4, the annual mean concentrations of TC were $2.4 \mu\text{gC m}^{-3}$ and $2.1 \mu\text{gC m}^{-3}$, which accounted for 19.5% and 22.6% of $\text{PM}_{2.5}$ concentrations in JFY 2015 and 2016, respectively. OC dominated over EC, and the annual mean OC/EC ratios were 2.6 and 3.2 in JFY 2015 and 2016, respectively. The ratio of OC/EC is often used as an indicator of the sources for the carbonaceous aerosol. We compared the annual mean OC/EC ratios between the Niigata-Maki site with those at some urban sites in Yokohama (Khan *et al.*, 2010), Chiba (Ichikawa *et al.*, 2015) and Kameda (MOEJ, 2016) in Japan. The annual mean OC/EC ratios at the Niigata-Maki (2.6 and 3.2 in JFY 2015 and 2016) were higher than those at the urban sites of Yokohama (1.9), Chiba (2.5) and Kameda (2.2). The Niigata-Maki site is classified as a rural site where there is no significant stationary source and low vehicular traffic. Because EC is considered as a tracer of diesel emission or fossil fuel combustion of stationary sources, the higher OC/EC ratio at the Niigata-Maki also represented the characteristics of a rural site.

The seasonal EC and OC concentrations were summarized in Table 4. EC concentration showed no strong seasonal variation. However, clear seasonal variation of OC was observed at the Niigata-Maki site. The seasonal mean concentrations of OC were in the order of spring > summer > autumn > winter during JFY 2015 and 2016. This result is similar to the results of some previous observational studies in Japan. For examples, the contribution of secondary formation, especially in summer, is more important for organic aerosols in Saitama, a suburban area of Tokyo (Bao *et al.*, 2009). Moreover, the seasonal average contributions of secondary OC to total OC in $\text{PM}_{<2.1}$ were 60%, 75%, and 36% in spring, summer, and winter in Gunma Prefecture, a suburban area of Tokyo, respectively (Kumagai *et al.*, 2010). The high contributions of secondary OC are attributable to high photochemical oxidant concentrations (>100 ppb). The observed high OC concentrations in spring and summer may result from higher temperatures and more intense solar radiation, which provide favorable conditions for photochemical activity and secondary OC production (Khan *et al.*, 2010).

3.2.3 Metallic elements analysis

In this study, 23 metallic elements (Al, Fe, Ni, Cr, Zn, Mn, Co, Cu, V, Ga, As, Se, Rb, Sr, Sc, Mo, Cd, Sb, Cs, Ba, Pb, Ag and Hg) in PM_{2.5} were also measured during sampling period. The seasonal and annual mean concentrations and the crustal enrichment factor (EF) for each elements is summarized in Table 5. The *EF* has commonly been used as a first step in attempting to evaluate the strength of the crustal versus anthropogenic sources, defined as:

$$EF = ([Z]_{\text{aerosol}}/[Al]_{\text{aerosol}})/([Z]_{\text{crust}}/[Al]_{\text{crust}}), \quad (7)$$

Where $[Z]_{\text{aerosol}}$ and $[Al]_{\text{aerosol}}$ are the target elements and aluminum concentrations in PM_{2.5}, and $[Z]_{\text{crust}}$ and $[Al]_{\text{crust}}$ are the reference concentrations of target elements and aluminum in crustal material (Alekseenko, 2014), respectively. If $EF < 2$, crustal soils are likely the predominant source for element, and if $EF > 5$ it suggests strong enrichment from non-crustal sources (Gao *et al.*, 2002). The *EF* values in overall period (Mn, 1.65; Rb, 1.26; Sr, 0.43; Cs, 0.87 and Ba, 1.81) were lower, which suggests those elements were mainly from crustal sources. Since the *EF* of aluminum with respect to rubidium (Rb) is less than 1, aluminum is also mainly originated from crustal sources. The EFs for Ni, Cr, Se, Mo and Sb were obviously high (183, 116, 2445, 600 and 437) at Niigata-Maki site, which indicates that PM_{2.5} is highly enriched by these metallic elements. Previous studies showed that the EFs of Ni, Cr, Se, Mo and Sb were higher (65, 32, 12300, 1370 and 20900) than other metallic elements in Tokyo. Furuta *et al.*, (2005) suggested that Ni and Cr were originated from chemical industry sources, and Sb was from the combustion of plastic products and brake pad wear of automobiles. The EFs of Ni, Cr, Se were also high (55, 35, 6698) at the Hachimantai mountain range in northern Japan. This result suggested that Cr was originated from industrial sources, and the Se was from coal combustion or exhaust of vehicles (Kikuchi *et al.*, 2010). These previous studies can be used for references to identify anthropogenic emission sources of the high EFs elements.

As shown in Table 5, the annual mean concentrations of a total 23 metallic elements were

702.3 ng m⁻³ (JFY 2015) and 279.2 ng m⁻³ (JFY 2016), which were 5.7% and 3.0% of the annual means of PM_{2.5} at Niigata-Maki site, respectively. The concentrations of iron (Fe) and aluminum (Al) were highest among 23 metallic elements in PM_{2.5}. The major metallic elements Al and Fe to total metallic elements were accounted for 24.2% and 51.6% at Niigata-Maki site in JFY 2015, and 52.4% and 29.2% in JFY 2016, respectively. No obvious seasonal variation of metallic elements was observed, but we found a remarkably high concentration event of Fe, Ni and Cr in winter JFY 2015. These metallic elements were recommended as markers for the metal processing industry, especially for steel works (Chen *et al.*, 2014). The waste incineration was also a source of Ni and Cr (Reimann *et al.*, 1998).

Table 5. Seasonal mean concentrations of metallic elements in PM_{2.5} at Niigata-Maki. (N.D. = Not Detected).

Season	Al	Fe	Ni	Cr	Zn	Mn	Co
	ng m ⁻³						
JFY 2015 Spring	283±386	186±175	3.45±5.01	5.10±2.07	N.D.	7.63±8.26	0.12±0.10
Summer	88.7±39.6	144±93.5	19.9±18.3	6.47±1.95	1.68±6.30	4.37±2.40	0.29±0.70
Autumn	71.6±45.8	77.6±26.9	22.5±24.5	5.01±1.47	N.D.	2.24±1.03	0.22±0.23
Winter	235±157	1037±1486	125±195	263±438	70.0±99.9	14.6±18.7	3.01±4.59
Annual mean	167±220	364±836	43.5±108	71.2±243	18.2±57.9	7.19±11.1	0.93±2.59
JFY 2016 Spring	171±29.8	36.8±22.4	6.15±6.38	4.08±1.61	5.74±13.0	1.73±1.22	0.04±0.04
Summer	70.8±71.5	48.9±35.5	7.12±6.11	5.85±2.68	27.4±59.3	2.17±1.32	0.10±0.16
Autumn	262±227	136±64.2	7.65±7.06	4.19±2.44	N.D.	4.50±2.45	0.04±0.02
Winter	59.5±29.0	91.9±37.8	3.08±6.64	5.56±2.20	7.46±19.7	1.69±1.27	0.32±0.69
Annual mean	144±152	82.4±59.05	6.06±6.64	4.93±2.36	10.9±33.1	2.63±2.05	0.13±0.36
EF Value	0.79 ^a	2.45	183	116	22.6	1.65	9.19
Season	Cu	V	Ga	As	Se	Rb	Sr
	ng m ⁻³						
JFY 2015 Spring	3.03±1.59	3.33±3.22	0.51±0.49	1.46±1.06	0.92±0.60	0.64±0.65	1.14±1.49
Summer	4.80±2.43	4.66±3.40	0.79±1.84	0.93±1.10	1.05±0.78	0.30±0.16	1.11±0.68
Autumn	1.81±0.62	0.52±0.16	0.51±0.48	0.59±0.47	0.34±0.19	0.30±0.10	0.46±0.24
Winter	7.78±10.5	1.67±1.85	0.48±0.25	0.68±0.48	0.31±0.33	0.33±0.17	0.88±0.40
Annual mean	4.38±5.82	2.53±2.91	0.57±1.00	0.91±0.88	0.65±0.61	0.39±0.36	0.89±0.85
JFY Spring	1.58±1.47	2.42±2.76	0.08±0.10	0.70±0.44	0.38±0.25	0.21±0.15	0.29±0.24
Summer	3.33±2.85	1.64±0.92	0.51±1.25	0.61±0.33	0.52±0.29	0.17±0.13	0.80±0.69

2016 Autumn	2.37±1.81	0.38±0.24	1.49±0.57	0.46±0.57	0.29±0.22	0.29±0.16	1.14±0.93
Winter	1.16±0.61	0.38±0.17	0.37±0.22	0.39±0.45	0.26±0.20	0.20±0.17	0.47±0.39
Annual mean	2.14±2.00	1.13±1.56	0.61±0.53	0.54±0.46	0.36±0.26	0.22±0.15	0.71±0.71
EF Value	20.4	4.27	9.36	11.07	2445	1.26	0.43
Season	Sc	Mo	Cd	Sb	Cs	Ba	Pb
	ng m ⁻³						
Spring	0.78±0.38	5.87±19.5	0.44±0.28	1.08±0.56	0.07±0.07	6.17±6.05	8.76±4.80
JFY Summer	0.68±0.57	0.68±0.31	0.20±0.16	1.06±0.90	0.03±0.02	9.85±26.2	6.06±4.60
2015 Autumn	0.49±0.25	0.63±0.20	0.09±0.04	5.67±6.90	0.02±0.01	6.13±9.88	7.32±13.5
Winter	0.95±0.68	2.14±2.96	0.13±0.16	1.37±1.00	0.02±0.02	3.85±3.55	4.31±3.64
Annual mean	0.72±0.60	2.27±9.55	0.21±0.22	2.32±3.90	0.03±0.03	6.51±14.3	6.57±7.75
Spring	N.D.	0.28±0.19	0.13±0.10	0.75±0.61	0.02±0.03	1.32±0.99	3.66±3.27
JFY Summer	N.D.	0.49±0.24	0.11±0.07	0.94±0.47	0.01±0.01	7.81±17.5	3.65±2.26
2016 Autumn	1.09±2.02	32.2±31.0	0.55±1.10	0.63±0.60	0.01±0.01	10.2±9.19	4.04±3.57
Winter	0.23±0.73	0.17±0.12	0.09±0.10	2.74±4.15	0.01±0.02	3.70±1.68	4.62±5.39
Annual mean	0.37±1.21	9.51±21.8	0.24±0.62	1.26±2.25	0.01±0.02	6.11±10.4	4.01±3.71
EF Value	12.8	600	59.7	437	0.87	1.81	23.7

The values after “±” denote standard deviations based on daily mean concentrations.

^aEF of aluminum is calculated by $([Z]_{\text{aerosol}}/[Rb]_{\text{aerosol}})/([Z]_{\text{crust}}/[Rb]_{\text{crust}})$.

The concentrations of Ag and Hg were under detection limits during sampling periods, and thus they were not shown in Table 5.

3.2.4 Contribution of Chemical components between $PM_{2.5}$ and $PM_{>2.5}$ in ambient air

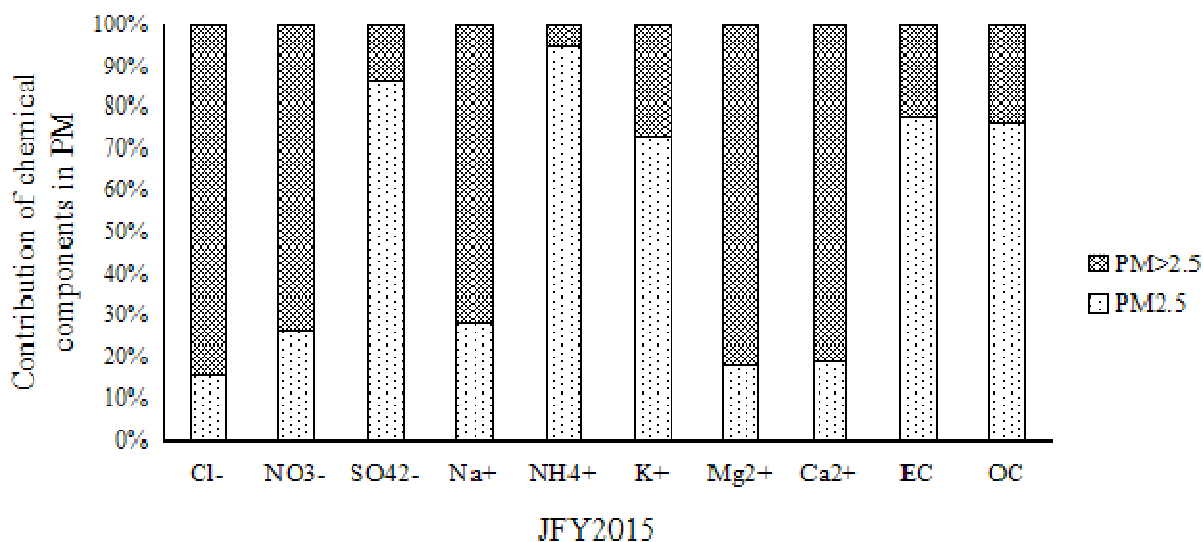
$PM_{>2.5}$ samples were also collected by using a high volume sampler (HV-1000F, Sibata Scientific Technology Ltd., Japan) during the same sampling period of $PM_{2.5}$ at Maki site. This study was carried out to characterize the contribution of water-soluble ions and carbonaceous in $PM_{2.5}$ and $PM_{>2.5}$ in ambient air, which the concentrations and contributions of chemical components are shown in Table 6 and Fig. 7. The dominant species in $PM_{2.5}$ were SO_4^{2-} , NH_4^+ , K^+ , OC and EC, which respective ratio in SO_4^{2-} , NH_4^+ , K^+ , OC and EC of PM were 86.45%, 94.37%, 73.08%, 76.18% and 77.55% in JFY2015, and respective ratio in SO_4^{2-} , NH_4^+ , K^+ , OC and EC of PM were 83.14%, 97.52%, 78.63%, 81.34% and 90.85% in JFY2016. The results obtained in this study also showed that the Cl^- , Na^+ , NO_3^- , Mg^{2+} and Ca^{2+} are largely confined to

the coarse fractions ($PM_{>2.5}$), which respective ratio in SO_4^{2-} , NH_4^+ , K^+ , OC and EC of PM were 84.16%, 71.67%, 73.56%, 81.63% and 80.62% in JFY2015, and respective ratio in SO_4^{2-} , NH_4^+ , K^+ , OC and EC of PM were 89.18%, 78.59%, 55.49%, 79.80% and 67.32% in JFY2016.

These analyses of the obtained results showed that secondary and carbonaceous aerosols are associated mostly with $PM_{2.5}$, while the Cl^- , Na^+ , Ca^{2+} and Mg^{2+} are dominated to the coarse particulate matter ($PM_{>2.5}$).

Table 6. Annual mean concentrations of water-soluble ionic species, OC and EC at Niigata-Maki.

Annual mean		Cl^-	NO_3^-	SO_4^{2-}	Na^+	NH_4^+	K^+	Mg^{2+}	Ca^{2+}	EC	OC
		$\mu g m^{-3}$	$\mu g C m^{-3}$	$\mu g C m^{-3}$							
JFY2015	$PM_{2.5}$	0.37	0.36	3.81	0.52	1.22	0.22	0.03	0.04	0.66	1.78
	$PM_{>2.5}$	1.97	1.00	0.60	1.32	0.07	0.08	0.13	0.17	0.19	0.56
JFY2016	$PM_{2.5}$	0.25	0.34	2.01	0.32	0.7	0.14	0.03	0.03	0.49	1.61
	$PM_{>2.5}$	2.06	0.42	0.41	1.17	0.02	0.04	0.12	0.06	0.05	0.37



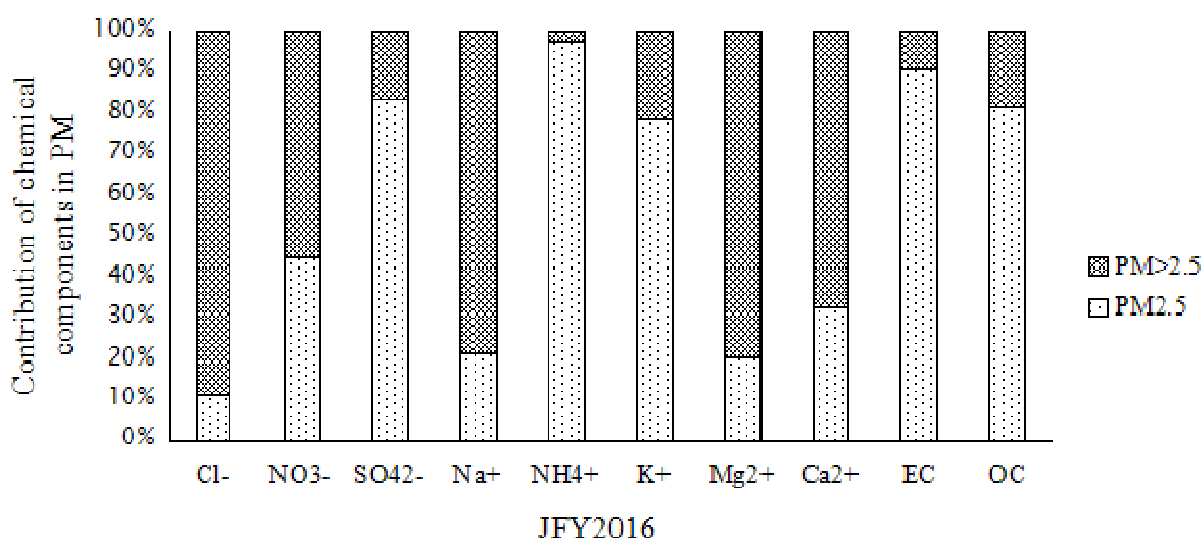


Fig. 7. Contribution of chemical components in PM

3.3 $PM_{2.5}$ mass balance

Summation of determined major chemical components (SO_4^{2-} , NO_3^- , Cl^- , NH_4^+ , Na^+ and EC) and estimated fraction (Organic carbon matter (OCM) and soil dust) were compared with $PM_{2.5}$ mass concentration to evaluate whether the mass balance discrepancy was significant. The following equation was used to estimate OCM including O, H, N compounds:

$$OCM = k (OC_m - OC_b) \quad (8)$$

Where OCM is organic carbon matter; k is adjustment factor to account for non-carbon organic matter (1.4) (Bell *et al.*, 2007); OC_m is measured organic carbon; OC_b is organic carbon for blank filters. Conversion of OC to OCM ($\pm 33\%$), varies with aerosol type and mix, volatile or other OC may pass through Teflon, therefore the uncertainty of k need to be estimated.

Soil dust was estimated from the measured concentrations of Al, Mg, K, Ca, Fe, and the estimated concentration of Si. The silicon concentration was estimated from the average mass ratio of Si to Al in the earth's crust as $Si = 3.41Al$ (Mason, 1966), the concentration of soil dust was calculated with the following equation (Hueglin *et al.*, 2005).

$$Soil\ dust = 1.89Al + 1.66Mg + 1.21K + 1.40Ca + 1.43Fe + 2.14Si \quad (9)$$

Fig. 8 shows the mass balance between the $PM_{2.5}$ mass and the sum of the aerosol chemical components. The annual means $PM_{2.5}$ mass was 6.2% and 17.0% larger than the sums of the aerosol chemical components in JFY 2015 and 2016, respectively. The discrepancy between the $PM_{2.5}$ mass and the sums of the aerosol chemical components varies among different seasons, and the $PM_{2.5}$ mass exceeded maximum 30.8% in spring JFY 2016. On the other hand, the $PM_{2.5}$ mass was maximum 29.5% lower than the sum of the aerosol chemical components in winter JFY2015. This can be explained by the remarkably higher concentration of Fe. The EF value of Fe was 7.56 in winter JFY 2015, which implies that a significant portion of Fe was originated from anthropogenic sources. Since all of Fe measured concentrations were calculated soil dust by the equation 5, the portion of soil dust was irregularly higher, and thus the sum of the aerosol chemical component exceeded the $PM_{2.5}$ mass in winter JFY 2015. Previous studies suggested that the mass balance discrepancy and its seasonal shift may be due to a combination of aerosol water content retained on the conditioned filters, and volatilization losses of $PM_{2.5}$ (Hering *et al.*, 1999; Pang *et al.*, 2002).

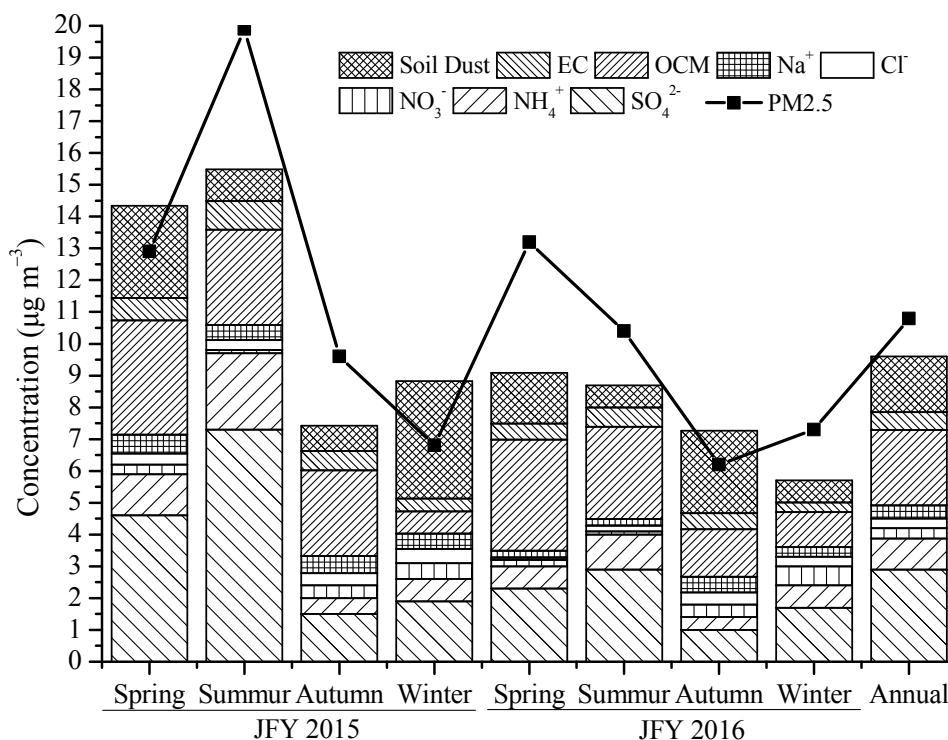


Fig. 8. Seasonal and annual discrepancy between the PM_{2.5} mass and the sums of the aerosol chemical components at Niigata-Maki. Annual is the average concentration of JFY2015 and 2016.

3.4 Major components of PM_{2.5}

Fig.8 shows annual average concentrations and annual average contributions of major components in PM_{2.5} at Niigata-Maki site. The same data at Kameda, Chiba and Japan-average are also shown as references. As shown in Fig. 9 (b), water-soluble ions, OC and EC, which are major components of PM_{2.5}, accounted for 52.8%, 14.5% and 5.4% of the annual means PM_{2.5} mass concentration at Niigata-Maki site in JFY 2015, and accounted for 40.8%, 17.3% and 5.3% in JFY 2016, respectively. The sum of NO₃⁻, SO₄²⁻ and NH₄⁺ accounted for 82.0% and 80.6% of the water-soluble ions in JFY 2015 and 2016, respectively. The “Others” fraction is defined as PM_{2.5} mass concentration minus the sum of water-soluble ions, EC and OC concentrations. The others accounted for 27.3% and 36.6% of the annual means PM_{2.5} mass concentration in JFY2015

and 2016, respectively. This fraction is assumed to contain trace elements, organic matters other than carbon (OM), crustal elements of soil dust and analytical uncertainties of the measurement. OM was estimated by equation (8), $OM = OCM - OC$. Soil dust was estimated by equation (9). The annual sum of OM and soil dust accounted for 69.4% of the “Others” fraction, as shown in Fig. 8. These results showed that SO_4^{2-} , NO_3^- , NH_4^+ , OCM, EC and crustal elements were the major chemical components of $PM_{2.5}$ in Niigata.

We compared the mass concentration and the contributions of major components of $PM_{2.5}$ among Niigata-Maki, Kameda (MOEJ, 2016), Chiba (Ichikawa *et al.*, 2015) and Japan national average (MOEJ, 2016). As shown in Fig. 9(a), annual mean mass concentration of $PM_{2.5}$ at Niigata-Maki site was lower than Kameda, Chiba and Japan national average, and Chiba annual mean exceeded the annual JEQS mass concentration ($15 \mu g m^{-3}$). These results are probably due to respective site locations that Niigata-Maki is a rural site and Kameda is an urban site in Niigata, and that the Chiba site is located in Tokyo metropolitan area. The source categories of these regions are different, and the traffic source might be significant impact with urban site.

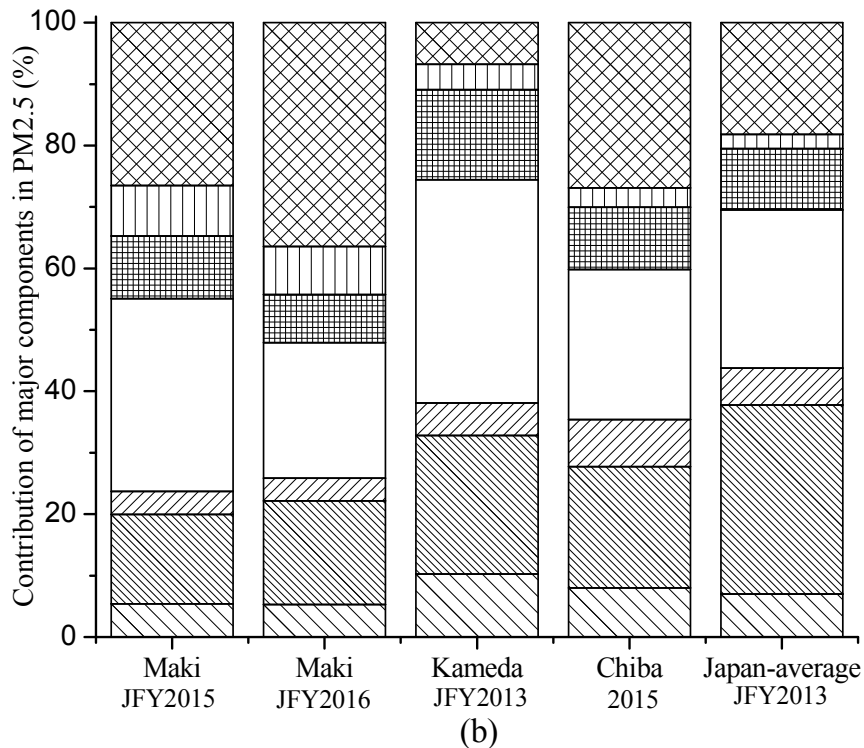
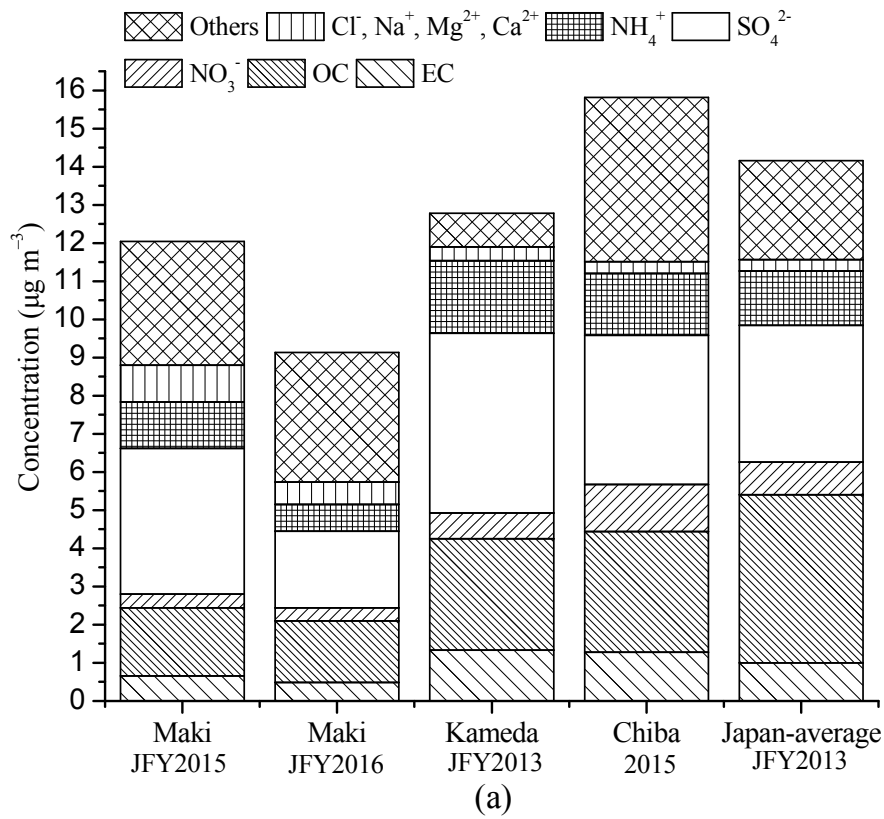


Fig. 9. (a) Annual average concentrations and (b) Annual average contributions of major components in PM_{2.5} at Niigata-Maki (JFY 2015 and 2016), Kameda (JFY 2013), Chiba (JFY 2015) and the Japan national average (JFY 2013). Others was calculated by subtraction of the PM_{2.5} mass concentrations from the sum of water-soluble ions, EC and OC concentrations.

As shown in Fig. 9(b), the ratio of total sea salt related ions of Cl^- , Na^+ , Mg^{2+} and Ca^{2+} to the $\text{PM}_{2.5}$ mass at Niigata-Maki (8.2% in JFY 2015, 7.8% in JFY 2016) was obviously higher than Kameda (4.1%), Chiba (3.1%) and Japan national average (2.3%), which is mainly due to the site location being close to the coast of the Sea of Japan. The ratios of EC to the $\text{PM}_{2.5}$ mass at Niigata-Maki (5.4% in JFY 2015, 5.3% in JFY 2016) were lower than at Kameda (10.3%), Chiba (8.0%) and Japan national average (7.0%), and the OC/EC ratios of Niigata-Maki (2.6 in JFY 2015, 3.2 in JFY 2016) were higher than Kameda (2.2), Chiba (2.5), which may be due to fewer traffic emission source near Niigata-Maki site. Since EC is an indicator of primary emission, diesel vehicle exhaust is probably the main source of EC in urban areas (Bao *et al.*, 2016). The ratios of NO_3^- to $\text{PM}_{2.5}$ mass at Niigata-Maki were obviously lower than Kameda and Chiba which also may be due to fewer traffic emission sources. The above differences showed that the contribution of vehicle source to $\text{PM}_{2.5}$ would be lower at the Niigata-Maki site, which the result is consist with Positive matrix factorization analysis in the section of source apportionment of $\text{PM}_{2.5}$.

3.5 Relationship between of $\text{PM}_{2.5}$ and meteorological factors

3.5.1 $\text{PM}_{2.5}$ concentration and meteorological factors

We compared the seasonal averages of $\text{PM}_{2.5}$ mass concentrations with various meteorological parameters of rainfall (mm), wind speed (m s^{-1}), and temperature ($^{\circ}\text{C}$). The meteorological data was obtained from the nearby monitoring station of the Japan Meteorological Agency (JMA) (JMA, 2017), which is located 6 km southeast of the Niigata-Maki station. As shown in Fig. 5, the seasonal variations of rainfall, wind speed and temperature might effect on the variation of $\text{PM}_{2.5}$ concentration. The higher seasonal $\text{PM}_{2.5}$ mass concentration is likely to be observed in the higher temperature, windless and less rainfall weather. These meteorological conditions corresponded to higher $\text{PM}_{2.5}$ concentrations in spring and summer. Previous studies

also showed that higher temperatures often enhance the chemical reactions of atmospheric pollutants (Zhang *et al.*, 2015; Sanchez-Romero *et al.*, 2014), that strong winds are favorable for the diffusion of air pollutants (Csavina *et al.*, 2014), and that PM_{2.5} was negatively correlated to the quantity of accumulated rainfall because of wet removal processes (Ouyang *et al.*, 2015).

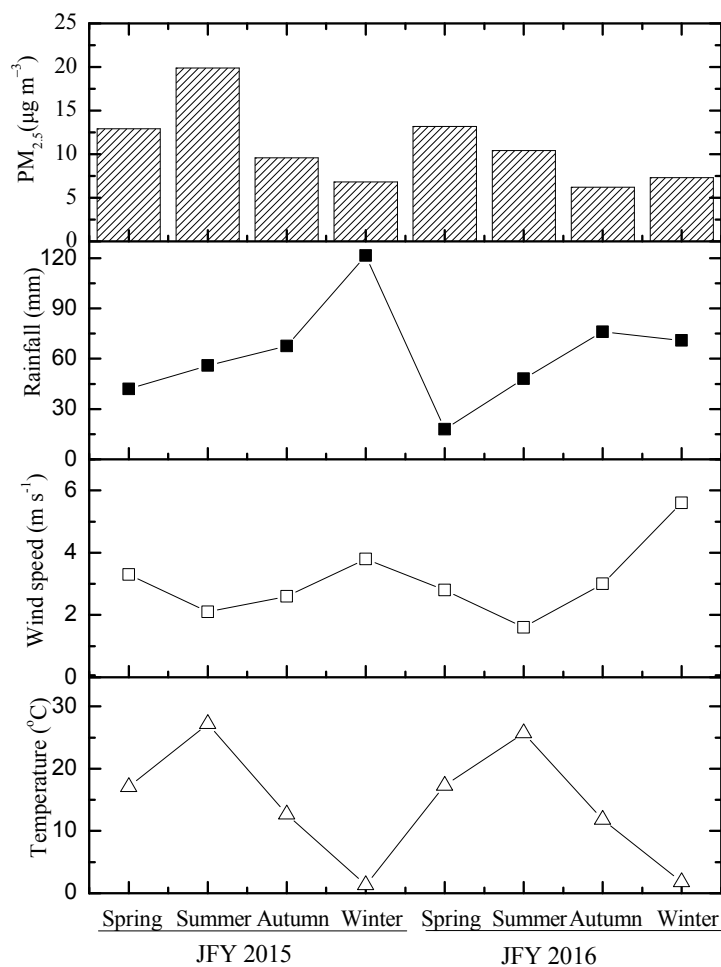


Fig. 5. Seasonal means of PM_{2.5} mass concentration, rainfall, wind speed and temperature at the Niigata-Maki and the near meteorological station.

Our previous study also showed Rainfall, relative humidity and wind speed were tightly responsible for the low PM_{2.5} concentration. The high PM_{2.5} mass concentration usually appeared with the Higher relative humidity, windless and less rainfall weather at Kameido site in urban Tokyo (Li *et al.*, 2017), as shown in Fig. 6.

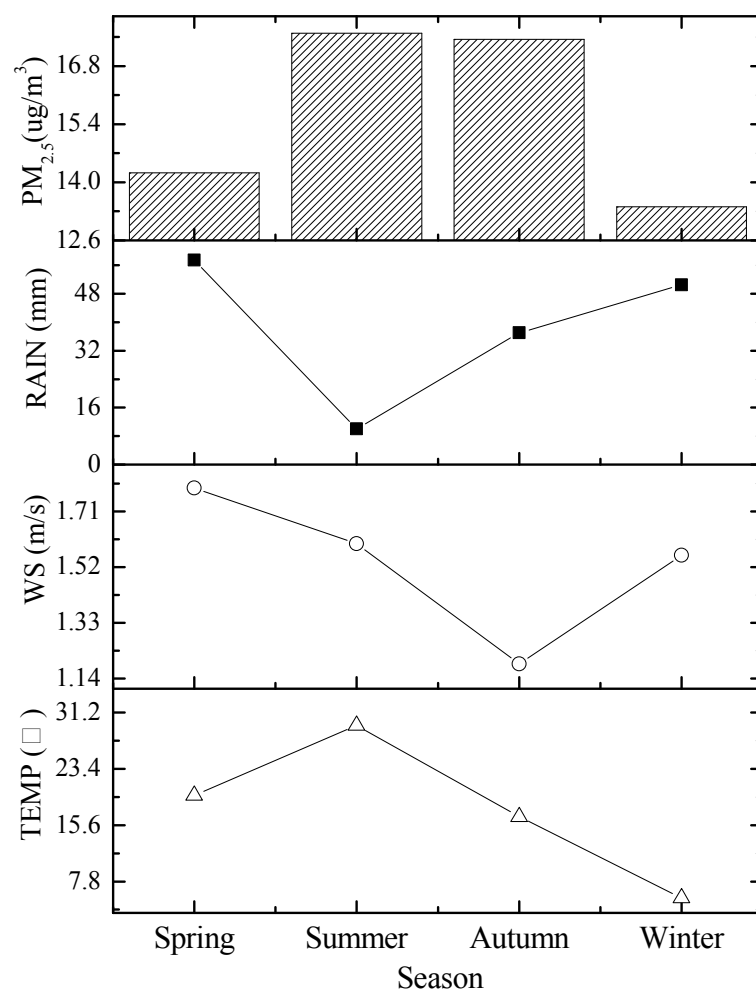


Fig. 6. Seasonal means of PM_{2.5} mass concentration, rainfall, wind speed and temperature at Kameido site in urban Tokyo.

3.5.2 Major components of PM_{2.5} and meteorological factors

To clear understand the relationships between meteorological factors and PM_{2.5} concentration, we calculated the spearman correlations between them, and it can be seen that some of the meteorological factors had correlations with PM_{2.5} concentrations from Table 7. Among these meteorological factors, the temperature had stronger correlations with PM_{2.5} concentrations than the other meteorological factors. The correlation coefficients were -0.619, 0.604, 0.577, 0.753, 0.690, 0.756 for NO₃⁻, SO₄²⁻, NH₄⁺, OC, EC and PM_{2.5} mass concentration respectively, their

p-values were all less than 0.001. Sunshine duration had stronger correlations with NO_3^- , SO_4^{2-} , Ca^{2+} , OC, EC and $\text{PM}_{2.5}$ mass concentrations, the correlation coefficients were -0.527, 0.412, -0.419, 0.669, 0.493, 0.516 and their p-values were less than 0.01, 0.05, 0.05, 0.01 and 0.01 respectively.

The significant positive correlation showed that increase of temperature and sunshine duration, the concentration of SO_4^{2-} , NH_4^+ , OC, EC and $\text{PM}_{2.5}$ mass concentration increased. Higher temperature and stronger sunshine duration were beneficial to chemical reaction of pollutants (Kang *et al.*, 2013; Yang *et al.*, 2016; Csavina *et al.*, 2014), therefore, the high temperature was beneficial to the formation of secondary aerosol, and obvious influence with $\text{PM}_{2.5}$ mass concentration in Niigata.

Relative humidity had stronger negative correlations with OC and mass concentrations of $\text{PM}_{2.5}$, the correlation coefficients were -0.828, -0.395 and their p-values were less than 0.01 and 0.05 respectively. Rain had stronger correlations with NO_3^- , OC, EC and $\text{PM}_{2.5}$ mass concentrations, the correlation coefficients were 0.556, -0.643, -0.572, -0.468 and their p-values were less than 0.01, 0.01, 0.01 and 0.05 respectively. Negative correlation showed that relative humidity and rain days were favorable for elimination of air pollutants. The above significant positive and negative correlations both had obvious statistical significance and certain practical implications.

Table 7. Relationships between meteorological factors and principal components of $\text{PM}_{2.5}$ in Niigata

	WS	TEMP	RH	RAIN	SUN
Cl ⁻	0.316	-0.170	-0.040	0.313	-0.265
NO_3^-	0.416*	-0.619**	0.224	0.556**	-0.527**
SO_4^{2-}	-0.055	0.604**	-0.311	-0.329	0.412*
Na^+	0.230	0.112	-0.218	0.121	0.039
NH_4^+	-0.117	0.577**	-0.240	-0.343	0.367
K^+	-0.208	0.296	-0.215	-0.107	0.171
Mg^{2+}	0.415*	-0.341	0.336	0.320	-0.348
Ca^{2+}	0.121	-0.314	0.276	0.211	-0.419*

OC	-0.431*	0.753**	-0.828**	-0.643**	0.669**
EC	-0.556**	0.690**	-0.357	-0.572**	0.493**
PM _{2.5}	-0.275	0.756**	-0.395*	-0.468*	0.516**

** . Correlation is significant at the 0.01 level .

* . Correlation is significant at the 0.05 level.

Comparing with our previous studies on the relationship between major components of PM_{2.5} and meteorological factors in urban Tokyo (Li *et al.*, 2017), as shown in Table 8. The significant correlation showed that increase of relative humidity, the concentration of NO₃⁻, SO₄²⁻, NH₄⁺, OC and EC increased. Higher relative humidity was beneficial to chemical reaction of pollutants. relative humidity and rain days were favorable for elimination of air pollutants. Higher temperature and stronger sunshine duration were beneficial to the formation of SO₄²⁻, but not conducive to the formation of NO₃⁻.

Table 8. Relationships between meteorological factors and major components of PM_{2.5} in urban Tokyo-Kameido site.

	WS	TEMP	RH	RAIN	SUN	NO ₃ ⁻	SO ₄ ²⁻	NH ₄ ⁺	OC	EC	PM _{2.5}
WS	1.00										
TEMP	0.08	1.00									
RH	-.39**	0.18	1.00								
RAIN	-0.22	-0.22	.64**	1.00							
SUN	.37**	.72**	-.36**	-.47**	1.00						
NO ₃ ⁻	-.69**	-.36**	.47**	.46**	-.59**	1.00					
SO ₄ ²⁻	-0.26	.47**	.47**	0.16	0.19	.29*	1.00				
NH ₄ ⁺	-.55**	0.10	.59**	.36**	-0.22	.69**	.81**	1.00			
OC	-.63**	0.22	.40**	0.11	-0.12	.48**	.59**	.66**	1.00		
EC	-.65**	0.08	.62**	.34**	-.27*	.71**	.53**	.78**	.73**	1.00	
PM _{2.5}	-.59**	0.20	.60**	.30*	-0.14	.62**	.79**	.92**	.83**	.85**	1.00

** . Correlation is significant at the 0.01 level.

* . Correlation is significant at the 0.05 level.

3.6 Correlations of chemical components in PM_{2.5}

Relationships between specific components could provide information about the sources of particles. If two elements show a good correlation, they are likely to be emitted from a similar source type. The Spearman correlation was carried out to investigate the relationship among chemical components in PM_{2.5}, shown in Table 9 and Table 10. In the analysis, only the correlations which are significant at the 1% level and these correlation coefficients (r) are more than 0.30 are considered. We found the following significant correlations and estimated the possible sources. The correlation coefficients among chemical components showed that:

a) Implications on secondary aerosol or combustion source origin: The SO_4^{2-} had significant correlation with NH_4^+ ($r = 0.94$), and the non-marine source results showed that the major sources of SO_4^{2-} (97%) in PM_{2.5} were mainly from anthropogenic sources. Therefore, this significant positive correlation revealed that SO_4^{2-} and NH_4^+ were attribute to a similar source type. NH_4^+ and SO_4^{2-} are known as tracer species of secondary aerosol to form $(\text{NH}_4)_2\text{SO}_4$. We found that SO_4^{2-} had also stronger correlation with K^+ ($r = 0.43$), V ($r = 0.59$), As ($r = 0.56$) and Se ($r = 0.75$). This suggested that $(\text{NH}_4)_2\text{SO}_4$ is related to combustion processes, because of K^+ is a marker of biomass burning source, V derive from oil combustion, and As and Se are potential sources of coal combustion. PM_{2.5} also had significant correlation with the major components SO_4^{2-} ($r = 0.85$), NH_4^+ ($r = 0.87$), and the metallic elements V ($r = 0.59$), As ($r = 0.53$) and Se ($r = 0.53$), as shown in Table 9. This implies that combustion processes are important to determine the PM_{2.5} mass level.

Table 9. Correlation matrix among PM_{2.5}, OC, EC, ionic species and metallic elements in PM_{2.5} at Niigata-Maki.

	PM _{2.5}	OC	EC	Cl ⁻	NO ₃ ⁻	SO ₄ ²⁻	Na ⁺	NH ₄ ⁺	K ⁺	Mg ²⁺	Ca ²⁺
PM _{2.5}											
OC	.56										
EC	.53	.61									
Cl ⁻											
NO ₃ ⁻											
SO ₄ ²⁻	.85	.35	.60								
Na ⁺				.82							
NH ₄ ⁺	.87		.62		.94						
K ⁺		.34	.41	.35	.43	.61	.39				
Mg ²⁺					.37	.32					
Ca ²⁺						.30		.39	.64		
V	.59				.59	.58					
As	.53	.42			.56	.57					
Se	.57	.43			.75	.70					
Pb	.30	.37									

Correlations which are significant at the 1% level and these correlation coefficients are more than 0.30 are shown in the table.

b) Implication on sea salt origin: The Na⁺ had stronger correlation with Cl⁻ ($r = 0.82$). Na⁺ ion in PM_{2.5} samples is mainly from sea salts, the significant positive correlation showed that Cl⁻ and Na⁺ were mainly from marine source. We also found that Mg had significant correlations with Ca ($r=0.640$), and Na⁺ had significant correlation with Mg²⁺ ($r = 0.32$) and Ca²⁺ ($r = 0.30$), moreover, the mean contributions of ss-Mg²⁺ and ss-Ca²⁺ in PM_{2.5} was estimated to be 86% and 66%, respectively. Therefore, Mg²⁺ and Ca²⁺ will also be mainly originated from sea salt.

c) Implication on biomass burning origin: EC had correlation with OC ($r = 0.61$) and K⁺ ($r = 0.41$) and OC with K⁺ ($r = 0.34$). These correlations were used to represent a biomass burning source. K⁺ was also a widely used tracer of biomass burning source (Ye *et al.*, 2003). Thus, EC, OC and K⁺ were formed into PM_{2.5} through biomass burning smoke.

Table 10. Correlation matrix among metallic elements species in PM_{2.5} at Niigata-Maki.

	Al	Fe	Ni	Cr	Zn	Mn	Co	Cu	V	Ga	As	Se	Rb	Sr	Sc	Mo	Cd	Sb	Cs	Ba	Pb	
Al																						
Fe	.78																					
Ni		.35																				
Cr		.50																				
Zn				.54																		
Mn	.72	.79																				
Co		.56	.36	.46		.45																
Cu	.44	.54	.32	.35		.72	.37															
V						.66		.68														
Ga	.58	.56				.49	.38															
As	.35	.31				.57		.51	.54	.33												
Se						.47		.46	.73	.74												
Rb	.55	.42			.46	.68		.45	.39	.36	.75	.64										
Sr	.75	.60		.32		.57		.49		.71	.40	.41	.47									
Sc	.50	.68		.31		.52																
Mo	.53	.54	.39	.42		.64	.32	.60		.49	.39		.39	.64								
Cd	.56	.39			.35	.66		.45	.67	.52	.59	.62	.75	.56		.46						
Sb							.41															
Cs	.51	.34				.59		.44		.40	.77	.69	.86	.48		.39	.77					
Ba	.46	.37				.31				.91				.65		.35	.52		.33			
Pb	.41					.58		.48		.33	.69	.69	.87	.40		.33	.76		.77			

Correlations which are significant at the 1% level and these correlation coefficients are more than 0.30 are shown in the table.

d) Implication on traffic or fossil fuel combustion origin: The high enrichment factor of (Ni, Cr, Zn, Co, Cu, V, As, Se, Rb, Sc, Mo, Cd, Sb, and Pb; EF > 5) suggests that the dominant sources for these metallic elements were non-crustal and a variety of pollution emissions may contribute to their loading in the ambient air. Significant correlations of these metallic elements are found in Table 10. Mn is an elemental marker for vehicular emissions, Mn and As are also emitted from road traffic generated particles (Wahlin *et al.*, 2006). Smelting (Cd, As, Pb, Zn, Cu and Sb), sewage sludge (As, Sn, Pb, Zn, Cu and Sb) and waste incineration (Sn and Pb) are also important pathways to primary emissions of particulate matter (Reimann *et al.*, 1998). The significant positive correlation showed that these elements were likely to be emitted from similar sources, and this possibly was attributed to the traffic, coal and oil combustion related sources.

3.7 Source apportionment of PM_{2.5} from PMF analysis

EPA PMF 5.0 was used to identify the potential sources of PM_{2.5}. The aim of PMF model is to minimize the function Q . Missing values were replaced by the median concentration of a given species, with an uncertainty of four times the median (Brown *et al.*, 2015). Values below method detection limit (MDL) are retained and related uncertainties are set at 5/6 of detection limit values. For values greater than the MDL, the calculation is based on a user provided fraction of the concentration and MDL, and the error fraction was suggested as 10% by the previous study of Paatero (2007). Uncertainty is defined as:

$$\text{Uncertainty} = \sqrt{(\text{ErrorFraction} \times \text{concentration})^2 + (0.5 \times \text{MDL})^2} \quad (10)$$

The number of factors to be chosen will depend on the user's understanding of the sources impacting samples, number of samples, sampling time resolution, and species characteristics. We run the PMF5.0 with moving the factors from two to seven, the decrease of Q/Q_{expected} is illustrated from 13.8 to 7.9, as well as a smaller decrease with moving from six to seven factors (8.4 to 7.9). When the changes in Q values become smaller than the increase of factors, it can suggest that there may be too many factors being fit (Brown *et al.*, 2015; Liu *et al.*, 2017). This result indicated that six factors may be the optimal solution.

The error estimation results of classical bootstrap (BS), displacement of factor elements (DISP), and bootstrap enhanced by displacement (BS-DISP), which is due to the small size of the data set and limited number of factors. The source apportionment results were generally stable at six factors, with all factors mapped in BS in 100% of runs except for the vehicle and industrial source factors (mapped on 85% and 81% of runs), mapping over 80% of the factors indicates that the BS uncertainties can be interpreted and the number of factors may be appropriate (PMF 5.0 User Guide, 2016). No swaps occurred with DISP also showed that the solution is stable, and all BS-DISP runs were successful. PM_{2.5} source apportionment was characterized by the following six factors, as shown in Fig. 10, and the contributions of each source to the PM_{2.5} mass was

shown in Fig. 11. Each factor could be characterized as follows.

Factor 1 was characterized by high positive loading of Cl^- (78.2%), NO_3^- (40.9%), Na^+ (64.2%), Mg^{2+} (71.1%) and Ca^{2+} (28.6%), which were mainly from sea salt. This result is consistent with the correlation result that Na^+ was significantly correlated with Cl^- , Mg^{2+} and Ca^{2+} , as shown in Table 9. The contributions of nss-SO_4^{2-} , nss-K^+ , nss-Ca^{2+} , nss-Mg^{2+} and nss-Cl^- in $\text{PM}_{2.5}$ calculated from the equation (2) also showed that 98% of Cl^- , 86% of Mg^{2+} and 66% of Ca^{2+} were from marine sources. Thus, the factor 1 was identified as sea salt, and its contribution to $\text{PM}_{2.5}$ was 10.2% as shown in Fig. 11.

Factor 2 was characterized by high positive loading of OC (85.9%), EC (52.9%) and K^+ (81.5%), which are generally considered as indicators of biomass burning, and K^+ is a widely used tracer of biomass burning source (Almeida *et al.*, 2015; Yao *et al.*, 2016). Thus, the factor 2 was identified as biomass combustion, and its contribution to $\text{PM}_{2.5}$ was 18.9%.

Factor 3 was characterized by high positive loading of Al (65.1%), Ga (54.8%), Sr (57.9%) and Ba (74.8%), which were mainly originated from crustal soil. As previously mentioned, the elements of $EF < 2$ suggest mainly natural crustal source origin, and those of $EF > 5$ suggest strong enrichment by non-crustal sources (Gao *et al.*, 2002). The mean EF values of these elements during overall period were very low (Al, 0.79; Ba, 1.81; and Sr, 0.43). This suggests that these elements are mainly originated from natural sources and mineral matter. It was also reported that trace elements of Ga and Sr are originated from re-suspension of road dust (Amato *et al.*, 2012). Thus, the factor 3 was identified as soil dust, and its contribution to $\text{PM}_{2.5}$ was 13.2%.

Factor 4 was characterized by high positive loading of major components of SO_4^{2-} (71.7%) and NH_4^+ (71.1%), and their typical source is secondary aerosol such as $(\text{NH}_4)_2\text{SO}_4$. Factor 4 was also represented by the high positive loading of metallic elements of V (69.4%), As (46.2%), Se (56.2%) and Pb (35.6%). V is a marker element of oil combustion (Okuda *et al.*, 2006), and As, Se and Pb are the typical anthropogenic sources of coal combustion (Reimann *et al.*, 1998; Wahlin *et al.*, 2006). Many PMF source apportionment studies have reported a relationship between

(NH₄)₂SO₄ and particulate matter components of combustion origin, such as heavy metals (Kim *et al.*, 2004). This is likely associated with SO₂ emissions from oil or coal-burning power plants forming secondary sulfate and reacting with gaseous NH₃ from a variety of sources. Thus, the factor 4 was identified as secondary aerosol and possibly associated with coal or oil combustion processes, and its contribution to PM_{2.5} was 44.4%.

Factor 5 was characterized by high positive loading of Zn (52.3%), Sb (53.1%), NO₃⁻ (50.8%), As (28.6%) and Pb (29.2%), and their typical source is vehicular traffic. Zn is a marker element of tire wear (Wahlin *et al.*, 2006), and Sb is known as a tracer of brake wear dusts (Iijima *et al.*, 2008, Iijima *et al.*, 2009). Mn and As are also emitted from re-suspension of road traffic-generated particles (Fabretti *et al.*, 2009). Pb is originated from tire dust or fuel combustion of vehicle (Smichowski *et al.*, 2008). Vehicular traffic is also a significant source of gaseous precursors (NO_x) and formed secondary aerosol of nitrate (de Gouw *et al.*, 2009). Thus, the factor 5 was identified as vehicular traffic, and its contribution to PM_{2.5} was 4.0%.

Factor 6 was characterized by high positive loading of Sc (92.9), Co (81.9%), Fe (62.9%), Cr (87.3%) Ni (86.5%), Cu (36.7%) and Mo (50.1%), which were possibly attributed to industrial activities. The common anthropogenic sources of Co, Cr, Ni, Cu and Fe include steel works and smelters. They are considered as markers for metal processing industry, especially for steel works (Chen *et al.*, 2014, Reimann *et al.*, 1998). Co and Ni are possibly originated from crude oil processing in refineries (Speight, 2014). Waste incineration is also a source of Ni and Cr (Reimann *et al.*, 1998). Thus, the factor 6 was identified as industrial activity, and its contribution to PM_{2.5} was 0.5%.

The PMF analysis demonstrated that the major sources of PM_{2.5} at the Niigata-Maki site were identified to be sea salt, biomass combustion, soil dust and secondary aerosol. Comparing with previous studies in western Japan, the major sources of PM_{2.5} in an industrial area of Hyogo Prefecture, located in the southern-central region of Honshu, were identified to be secondary sulfates (28.9%), vehicular traffic (20.8%), steel mills (7.8%), and secondary chloride and nitrate

(7.0%) (Nakatsubo *et al.*, 2014). The major sources of PM_{2.5} in Okinawa were identified to be coal combustion (32.6%), secondary species (28.5%), sea salt and nitrate (19.1%), oil combustion (12.8%), and soil dust (7.0%) (Shimada *et al.*, 2015). The high contribution of secondary aerosol was common between western Japan and our study, whereas low contribution of vehicular traffic and high contribution of biomass combustion in our study showed unique characteristics in the coast of the Sea of Japan. Indeed, our identified sources included both local and long range origin. In the next section, the significant origin area of the major sources of PM_{2.5} will be identified by the PSCF analysis.

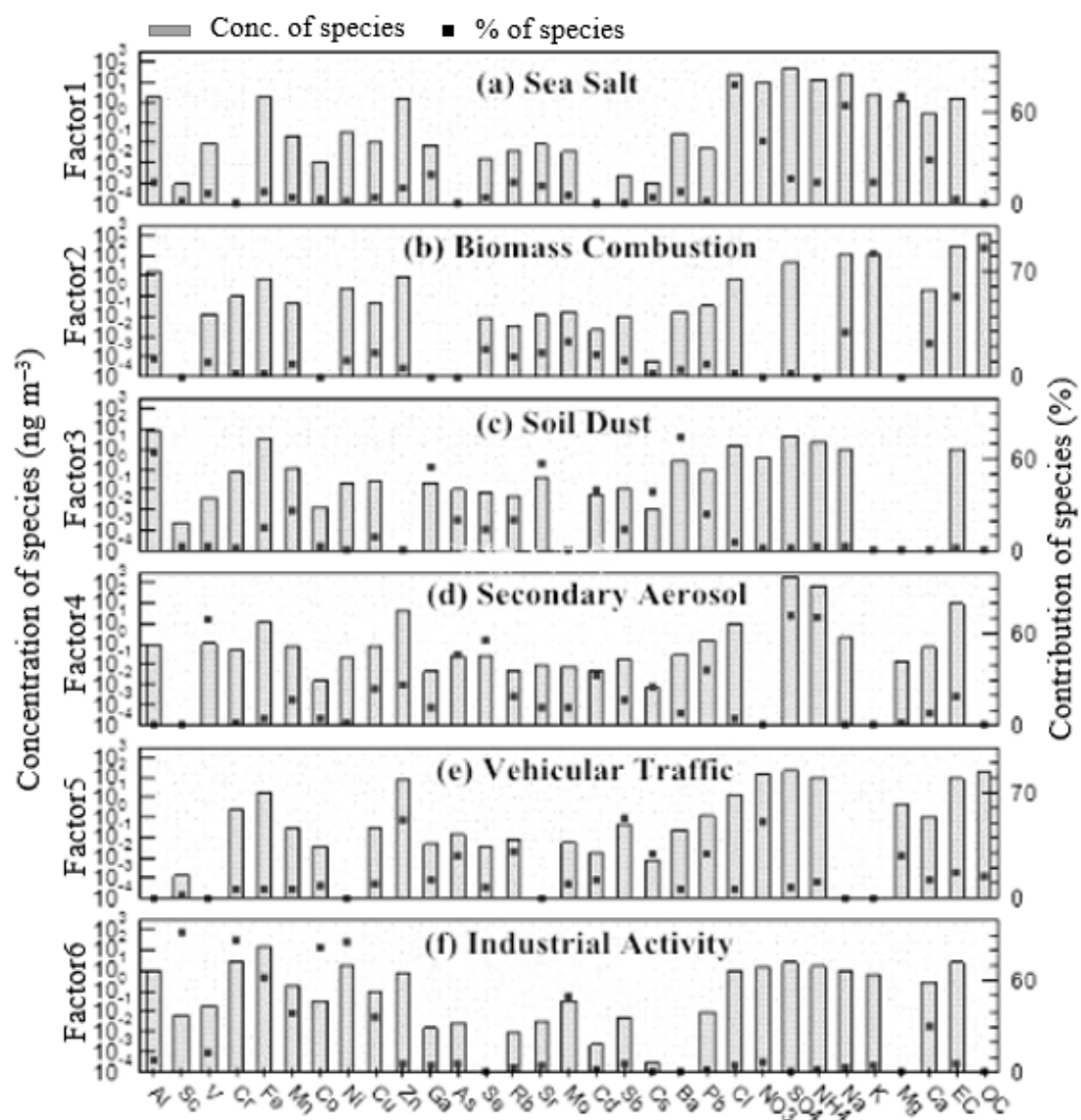


Fig. 10. Six factors obtained by using the PMF 5.0 model for each source category at Niigata-Maki: (a) sea salt, (b) biomass combustion, (c) soil dust, (d) secondary aerosol, (e) vehicular traffic, (f) industrial activity.

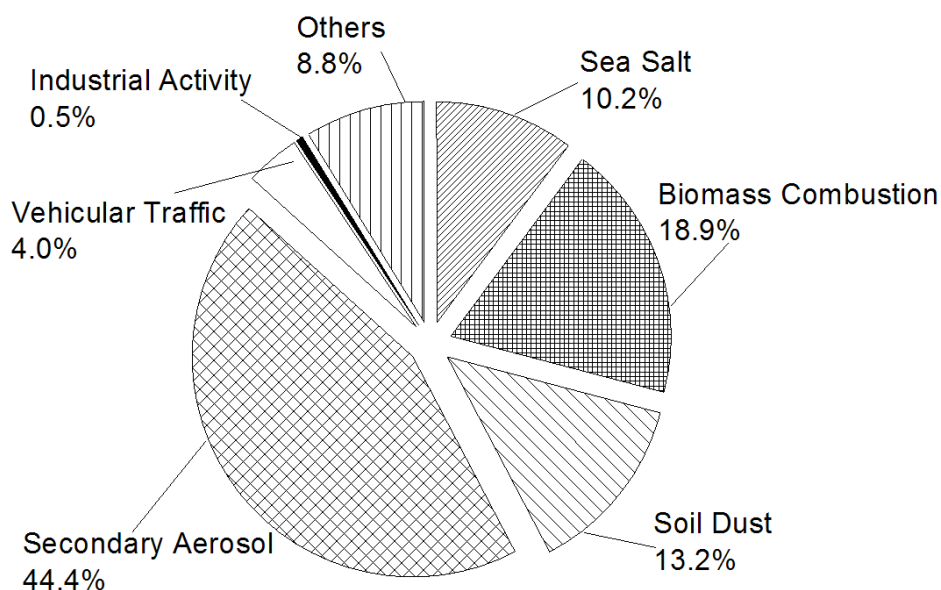


Fig. 11. The annual mean contribution of each source to the ambient $PM_{2.5}$ at Niigata-Maki.

3.8 Emission regions of $PM_{2.5}$ major sources by PSCF analysis

We performed the PSCF analysis to identify the preferred atmospheric transport pathways from sources to receptors by the Meteoinfo1.4.3: GIS-based software that uses various trajectory statistical analysis methods to identify potential sources from long-term air pollution measurement data (Wang *et al.*, 2009). 72-h backward trajectories were obtained by using the Meteoinfo1.4.3 model from the Global Data Assimilation System (GDAS) meteorological data (<ftp://gus.arlhq.noaa.gov/>). We used PSCF to estimate the back trajectories at arrival heights of 500, 1000, and 1500 m, and three-day back trajectories were used to calculate the PSCF values for $1^\circ \times 1^\circ$ grid cells computed for arrival heights of 500, 1000, and 1500 m for each of the 106 daily mean samples. The studying field is from 30 to 50 $^\circ N$, and 120 to 150 $^\circ E$, which includes more than 95% of area covered by all the paths. Regions with PSCF values ranging from 0.5 to 1 were designated as probable source regions for each factor during the study period. The potential source regions of the four major sources identified PMF analysis are shown in Fig. 12(a)-(d). The detailed discussions for respective sources are shown below.

Sea salt

Sea salt was characterized as major components of Cl^- , Na^+ , Mg^{2+} and Ca^{2+} by PMF analysis, Niigata-Maki station lies on the coast of the Sea of Japan, 1 km from the seashore, and thus, the high value PSCF plots suggested that Sea of Japan was the main source area of sea salt, as shown in Fig. 12 (a).

Biomass combustion

Biomass combustion source was characterized as major components of OC, EC and K^+ by PMF analysis. As shown in Fig. 12 (b), the high value PSCF plots suggested that local area in Niigata, southwest Japan, northeast China and Korea were the potential source areas. The biomass combustion emissions in the NEA are generally from agricultural waste burning after barley and wheat harvest (between late spring and early summer) and rice harvest (in the autumn) (Zang, 2015). Biomass burning activity in the NEA during these period were also estimated using a fire spot database, and the fire spots data are provided by the Fire Information for Resource Management System (FIRMS) (<https://firms.modaps.eosdis.nasa.gov/firemap/>), the satellite image in Fig. 13 showed dense hot spots appeared in northeast China in autumn during the sampling period. To better identify the potential sources of aerosols originating from these regions, we used seasonal fire spots to compare with the autumn biomass combustion PSCF plots (Fig. 14). The high dense regions of hotspot in autumn JFY 2015 and 2016 corresponded to high PSCF areas. These results showed that the major source of biomass combustion was from northeast China in autumn, and local area in Niigata and southwest Japan were the main source areas in the other seasons. Our previous study also showed high concentration episode of water insoluble organic carbon and EC in precipitation that is synchronized with high number of fire spots in the NEA, which implies considerable contribution of biomass combustion in spring and autumn (Huo *et al.*, 2016).

Soil dust

Crustal soil source was characterized as key elements of Al, Ga, Sr and Ba by PMF analysis. As shown in Fig. 12 (c), the high value PSCF plots suggested that local area in Niigata, northeast

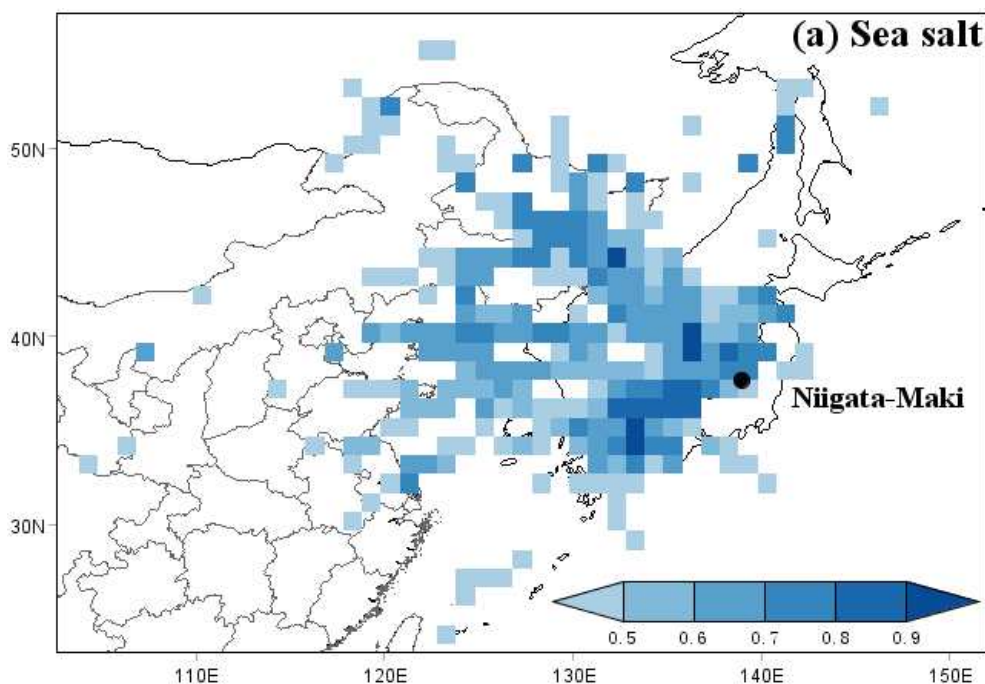
China, Korea and the Sea of Japan were the potential sources considering all seasons. When we focus on the seasonal soil dust PSCF plots in winter (Fig. 15), the major source area of soil dust was northeast China. For the other seasons, contributions of local area in Niigata and the Sea of Japan were more remarkable.

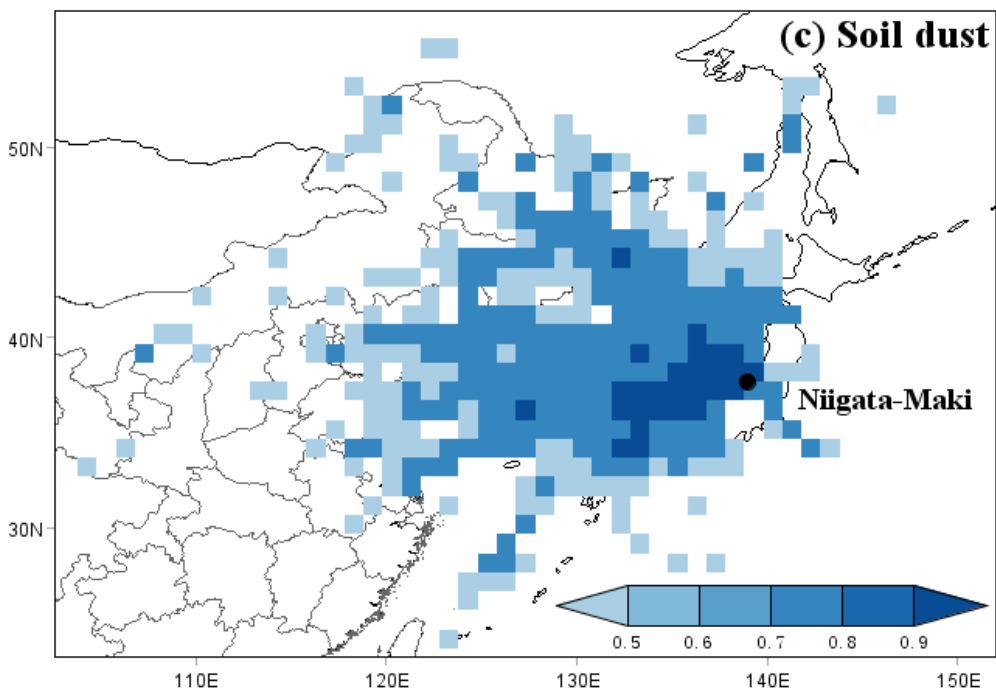
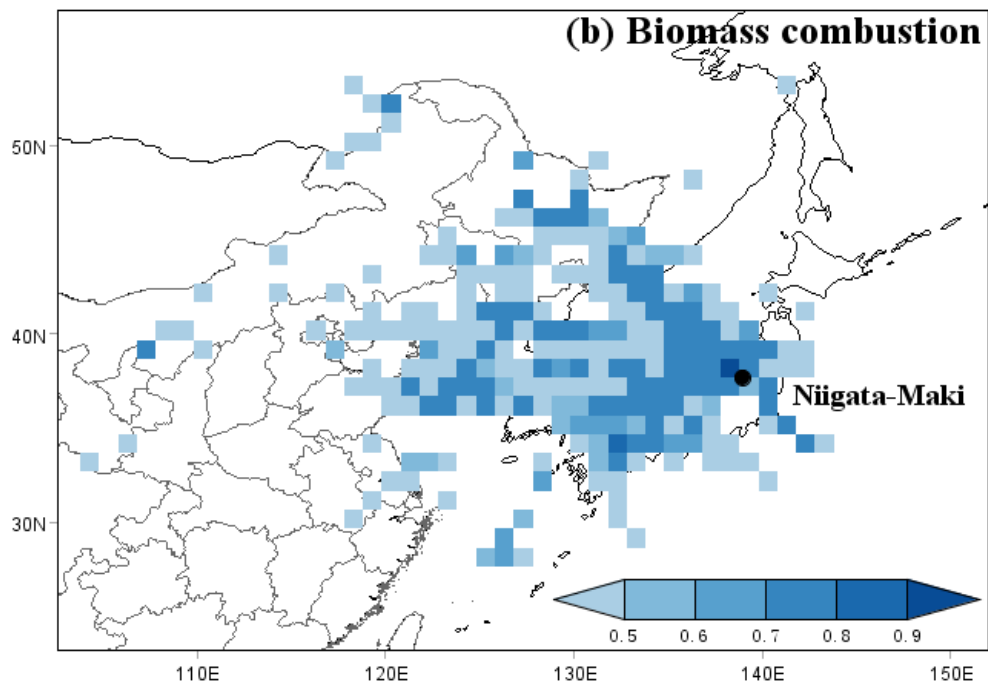
Secondary aerosol

Secondary aerosol was characterized as major components SO_4^{2-} and NH_4^+ by PMF analysis. As shown in Fig. 12 (d), the high value PSCF plots suggested that southwest Japan and Korea were the potential sources. The PMF source apportionment results showed a relationship between $(\text{NH}_4)_2\text{SO}_4$ and combustion origin. This was likely associated with SO_2 emissions from oil or coal burning power plants. Fig. 16 shows that the thermal power plants are concentrated in the southwest of Japan and Tokyo metropolitan area. Coal or oil burning factories and volcanoes were also the potential source of SO_4^{2-} in Japan, and Itahashi *et al.* (2017) revealed that the contribution of SO_4^{2-} originated from volcanoes is 28.7% in summer. The concentrations of SO_4^{2-} and NH_4^+ were obviously high in summer as shown in Table 4, when the Pacific high covers the mainland in Japan and the air mass is usually transported along the ridge of the Pacific high. Moreover, the central mountains in Japan seem to hinder transportation of air pollutants from Tokyo metropolitan area. In addition, for the summertime contribution of sulfate aerosol, many previous observation and numerical model simulation studies showed the large contribution from the Asian continent, especially China. For example, Aikawa *et al.* (2010) revealed the strong gradient of sulfate from west to east by comparing the observational data in several stations. This is the suggestion of long-range transport of sulfate aerosol over the Asian continent. The numerical modeling revealed that central China was the main SO_4^{2-} source region in China (Kajino *et al.*, 2011; Itahashi *et al.*, 2017). In Japan, the concentration of SO_4^{2-} was highest in summer and followed in spring, which the long range transportation of SO_4^{2-} from central China also had the great impact on sulfate concentration during the two seasons (Itahashi *et al.*, 2017). Ikeda *et al.* (2015) revealed that the relative contribution of China to the annual mean $\text{PM}_{2.5}$

concentration was estimated to be 50–60% in western Japan. Comparing with the previous studies showed that southwest Japan was the important source area contributing to secondary aerosol, which included local and long-range transport sources.

Table 4 also shows that the concentrations of SO_4^{2-} and NH_4^+ were higher in spring, and the back trajectory analysis results showed that the origins of the air masses arriving at Niigata-Maki were mainly from two regions (central China and southwest Japan), as shown in Fig. 17. Comparing with the above discussion on sulfate aerosol, which central China and southwest Japan were the important source areas in Japan. Therefore, it is also probable that the two regions had a greatly impact on secondary aerosols in Niigata during spring.





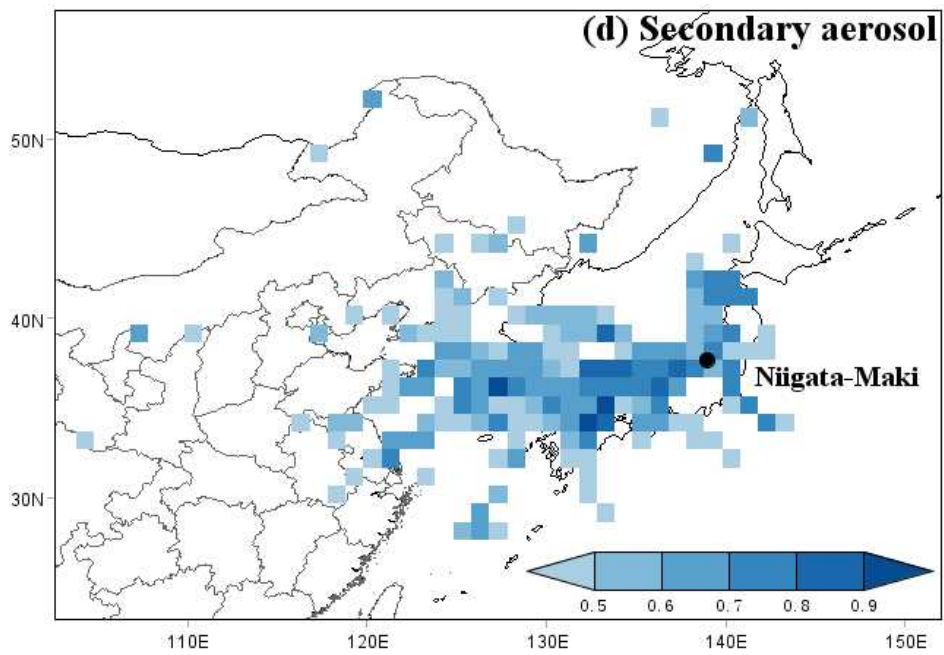


Fig. 12. Potential source regions by using PSCF analysis: (a) sea salt, (b) biomass combustion, (c) soil dust, (d) secondary aerosol.

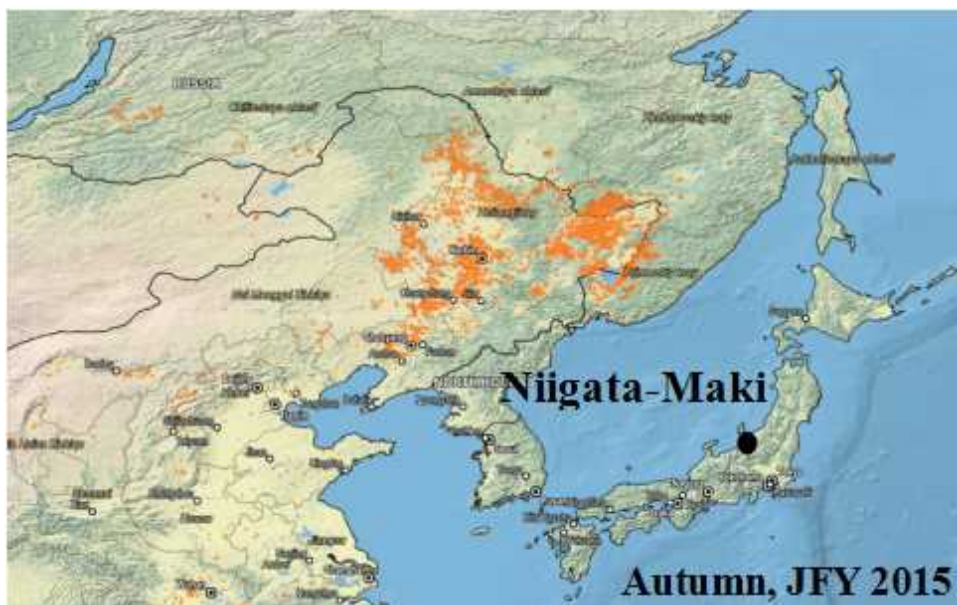




Fig. 13. Fire spots of biomass burning activity in spring and autumn in Northeast Asia from JFY 2015 to 2016 (<https://firms.modaps.eosdis.nasa.gov/firemap/>).

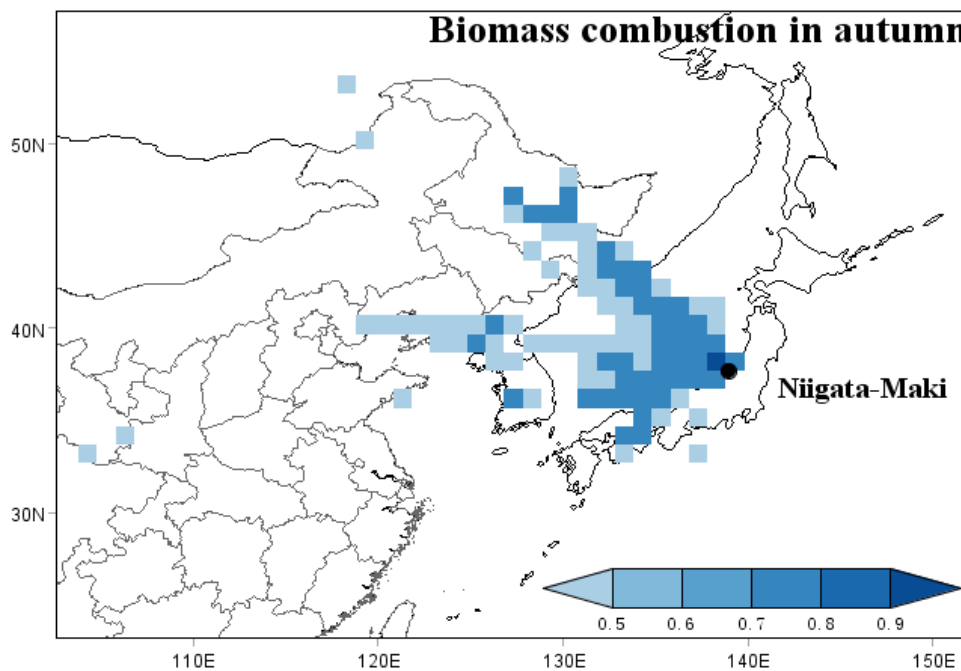


Fig. 14. Potential source regions of biomass combustion in autumn by using PSCF analysis at Niigata-Maki in JFY2015 and 2016.

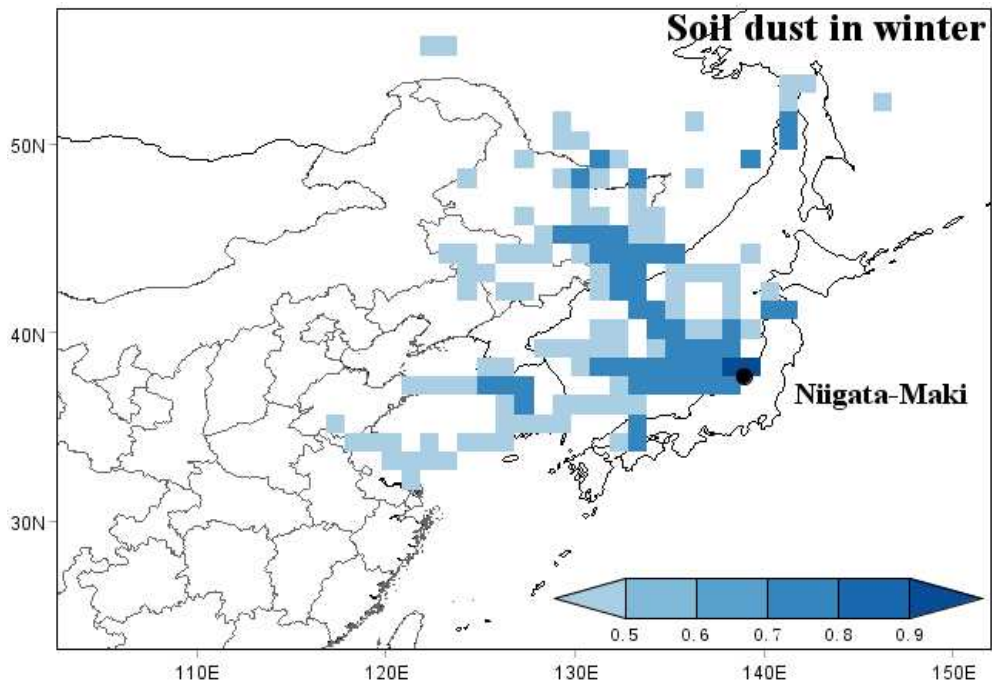


Fig. 15. Potential source regions of soil dust in winter by using PSCF analysis at Niigata-Maki in JFY2015 and 2016.

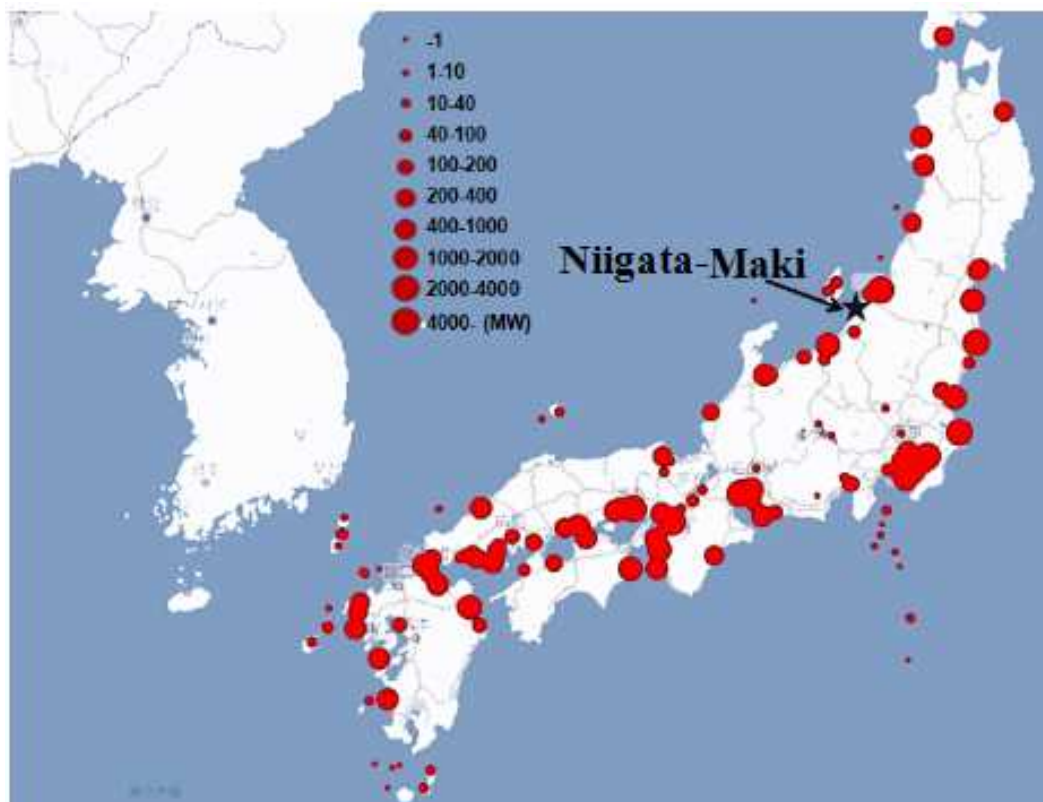
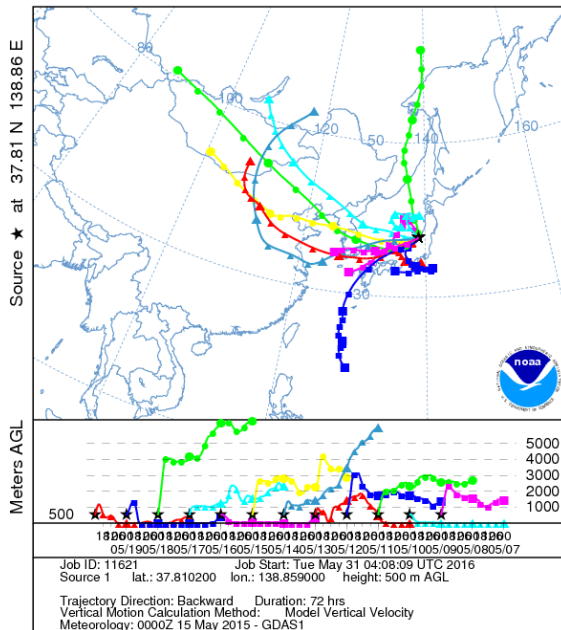


Fig. 16. Location of thermal power plants in Japan, referenced from (Electrical Japan, 2017).

NOAA HYSPLIT MODEL
 Backward trajectories ending at 0000 UTC 20 May 15
 GDAS Meteorological Data



NOAA HYSPLIT MODEL
 Backward trajectories ending at 0000 UTC 21 May 16
 GDAS Meteorological Data

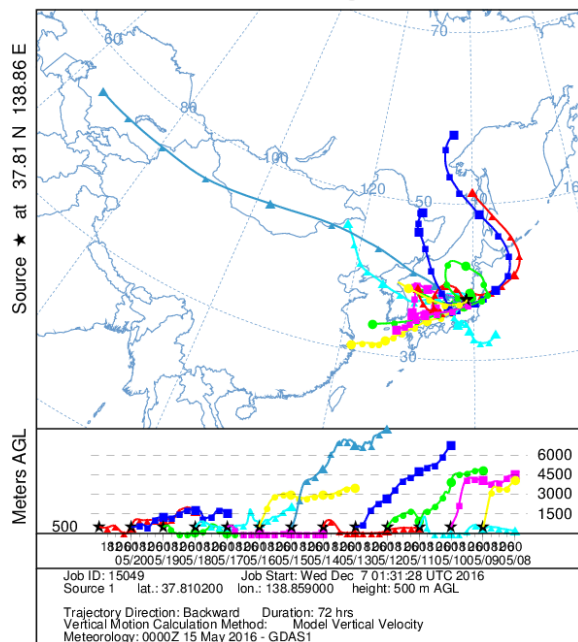


Fig. 17. The back trajectory analysis results in spring at Niigata-Maki site in JFY 2015 and 2016 (<http://www.arl.noaa.gov/index.php>).

The above results showed that the major sources of secondary aerosol and sea salts are domestic in southwest Japan and the Sea of Japan, whereas the sources of biomass combustion and soil dust in specific seasons are long range transportation from the NEA. Comparing with previous studies of PSCF analysis in urban area of western Japan (Nakatsubo *et al.*, 2014) and in remote area of southwestern Japan (Shimada *et al.*, 2015), this study showed a large domestic contribution of southwest Japan for secondary aerosol, while a larger contribution of the NEA was observed in previous studies. Moreover, significant contribution of biomass combustion originating from local or long-range transportation was observed on the coast of the Sea of Japan. This study showed the regional characteristics of PM_{2.5} sources in eastern Japan.

4. CONCLUSIONS

In this research, a field observation study including seasonal intensive measurement of PM_{2.5} was conducted from May 2015 to February 2017 at Niigata-Maki station in Niigata, eastern Japan. The annual mean mass concentrations of PM_{2.5} were 12.3 $\mu\text{g m}^{-3}$ (JFY 2015) and 9.3 $\mu\text{g m}^{-3}$ (JFY 2016). Daily mean concentrations of PM_{2.5} ranged from 4.2 $\mu\text{g m}^{-3}$ to 33.4 $\mu\text{g m}^{-3}$ at Niigata-Maki station during observation period, which were lower than Japanese Environmental Quality Standard for PM_{2.5} (35 $\mu\text{g m}^{-3}$ for daily average). PM_{2.5} concentration variation was highly correlated with meteorological conditions. We found that the higher seasonal PM_{2.5} mass concentration usually occurred with higher temperature, windless and less rainfall weather, such as during spring and summer. The higher concentrations of SO₄²⁻, NH₄⁺ and OC also observed in spring and summer may result from higher temperatures and more intense solar radiation, which provide favorable conditions for photochemical activity and secondary OC production. Annual average data showed that the major chemical components of PM_{2.5} were SO₄²⁻, NO₃⁻, NH₄⁺, OCM, EC and crustal elements. Comparing with the data at the urban sites of Kameda and Chiba, lower concentrations of EC and NO₃⁻ and higher OC/EC ratios were observed at the Niigata-Maki site. EC is considered as a tracer of diesel emission or fossil fuel combustion of stationary sources, and the vehicular traffic is also a significant source of gaseous precursors (NO_x) and formed secondary aerosol of nitrate. Therefore, the observational results suggested that there was no significant stationary source and low vehicular traffic around the site. The higher OC/EC ratio at the Niigata-Maki site is also representative of a rural site.

PM_{2.5} source apportionment was characterized by positive matrix factorization (PMF) analysis, and the results inferred four major emission sources: sea salt, biomass combustion, soil dust and secondary aerosol. The relative contributions of the four major sources to PM_{2.5} concentrations at Niigata-Maki were 10.2% for sea salt, 18.9% for biomass combustion, 13.2% for soil dust and 44.4% for secondary aerosol, respectively. We performed a potential source

contribution function (PSCF) analysis to identify potential source regions of the four major sources. The high value PSCF plots suggested that the Sea of Japan was the main source area of sea salt. The major source region of biomass combustion was from northeast China in autumn, and local areas in Niigata and southwest Japan were the main source areas in other seasons. The major source area of soil dust was northeast China in winter, while the contributions of local areas in Niigata and the Sea of Japan were more remarkable in other seasons. The secondary aerosol of $(\text{NH}_4)_2\text{SO}_4$ was mainly originated from southwest Japan. The PMF analysis and correlation results showed a relationship between $(\text{NH}_4)_2\text{SO}_4$ with oil or coal combustion source. Thermal power plants are concentrated in the southwest of Japan and Tokyo metropolitan area. Coal or oil burning factories and volcanoes were also the potential source of SO_4^{2-} in Japan. The concentrations of SO_4^{2-} and NH_4^+ were obviously high in summer, when the Pacific high covers the mainland in Japan and the air mass is usually transported along the ridge of the Pacific high. Moreover, the central mountains in Japan will hinder transportation from Tokyo metropolitan area. Therefore, southwest Japan was the major source region of secondary aerosol.

Comparing with previous source apportionment studies in western Japan, this study showed the regional characteristics of $\text{PM}_{2.5}$ sources at Niigata-Maki station in eastern Japan. A large domestic contribution from southwest Japan was observed for secondary aerosol, while a larger contribution of long-range transportation from the NEA was observed in previous studies. Significant contribution of biomass combustion from local or long-range transportation was uniquely observed. These results and scientific findings can be used for an evaluation of the atmospheric impact of $\text{PM}_{2.5}$ at Niigata-Maki station in eastern Japan.

Since few observation studies have focused on fine particles in a coastal city of Japan Sea in Eastern Japan, and long-range transportation across the coast of the Sea of Japan from the NEA, this comprehensive study of $\text{PM}_{2.5}$ is significance for the atmospheric environment science in Japan. Moreover, it can also provide a solid foundation for the systematic study of the long-range transportation of biomass combustion sources from NEA in the future.

ACKNOWLEDGMENTS

First of all, my thanks to prof. Hasegawa Hideo, my advisor, for all of the assistance and constructive advice and comments that he have provided throughout this work. I would like to thank my committee members: prof. Miguchi Hideo, prof. Nakata Makoto, prof. Matsuoka Shiro and Dr. Keiichi Sato for their invaluable advice and help in preparing this thesis. I am also grateful thank to Dr. Keiichi Sato, Dr. Hiroaki Minoura and Dr. Mingqun Huo in Asia Center for Air Pollution Research (ACAP), who provided the experiment conditions and a lot of important suggestion and advice for my work. Moreover, I am thankful for the help from members of ACAP as well, they all gave me so many supports for my work.

REFERENCES

- Almeida, S.M., Lage, J., Fernandez, B., Garcia, S., Reis, M.A. and Chaves, P.C. (2015). Chemical characterization of atmospheric particles and source apportionment in the vicinity of a steelmaking industry. *Sci. Total Environ.* 521-522: 411-420.
- Amato, F. and Hopke, P.K. (2012). Source apportionment of the ambient PM_{2.5} across St. Louis using constrained positive matrix factorization. *Atmos. Environ.* 46(3): 329–337.
- Bao, L., Sekiguchi, K., Wang, Q. and Sakamoto, K. (2009). Comparison of Water-Soluble Organic Components in Size-Segregated Particles between a Roadside and a Suburban Site in Saitama, Japan. *Atmos. Environ.* 9: 412-420.
- Bell, M.L., Dominici, F., Ebisu, K., Zeger, S.L. and Samet, J.M. (2007). Spatial and Temporal Variation in PM_{2.5} Chemical Composition in the United States for Health Effects Studies. *Environmental Health Perspectives* 115(7): 989-995.
- Chan, C.C., Chuang, K.J., Chien, L.C., Chen, W.J. and Chang, W.T. (2006). Urban air pollution and emergency admissions for cerebrovascular diseases in Taipei, Taiwan. *Eur. Heart J.* 27 (10): 1238-1244.
- Chen, Y., Schleicher, N., Chen, Y., Chai, F. and Norra, S. (2014). The influence of governmental mitigation measures on contamination characteristics of PM_{2.5} in Beijing. *Sci. Total Environ.* 490: 647-658.
- Cheng, Z., Wang, S., Jiang, J., Fu, Q., Chen, C., Xu, B., Yu, J., Fu, X. and Hao, J. (2013). Long-term trend of haze pollution and impact of particulate. *Environmental Pollution* 182: 101–110.
- Chow, J.C., Watson, J.G., Crow, D., Lowenthal, H.D. and Merrifield, T. (2001). Comparison of IMPROVE and NIOSH Carbon Measurements. *Aerosol Sci. Technol.* 34: 23–34.
- Coulibaly, S., Minami, H., Abe, M., Hasei, T., Oro, T., Funasaka, K., Daichi, A., Masanari, W., Naoko, H., Keiji, W. and Watanabe, T. (2015). Long-range transport of mutagens and other

- air pollutants from mainland East Asia to western Japan. *Genes and Environ.* 37 (1): 1-10.
- Csavana, J., Field, J., Felix, O., Alba, Y., Avitia, C., Saez, A.E. and Betterton, E.A. (2014). Effect of wind speed and relative humidity on atmospheric dust concentrations in semi-arid climates. *Sci. Total Environ.* 487: 82–90.
- de Gouw, J. A. and Jimenez, J. L. (2009). Organic Aerosols in the Earth's Atmosphere. *Environ. Sci. Technol.* 43: 7614–7618.
- Electrical Japan, <http://agora.ex.nii.ac.jp/earthquake/201103-eastjapan/energy/electrical-japan/type/1.html.ja>. Last Access: 21 April 2017.
- Fabretti, J.-F., Sauret, N., Gal, J.-F., Maria, P.-C. and Schärer, U. (2009). Elemental characterization and source identification of PM_{2.5} using positive matrix factorization: the Malraux road tunnel, Nice, France. *Atmos. Res.* 94 (2): 320–329.
- Furuta, N., Iijima, A., Kambe, A., Sakai, K. and Sato, K. (2005). Concentrations, enrichment and predominant sources of Sb and other trace elements in size classified airborne particulate matter collected in Tokyo from 1995 to 2004. *J. Environ. Monit.* 7(12):1155-61.
- Gao, Y., Nelson, D.E., Field, P.M., Ding, Q., Li, H., Sherrell, R.M., Gigliotti, C.L., Ryda, V., Glenn, T.R. and Eisenreich, S.J. (2002). Characterization of Atmospheric Trace Elements on PM_{2.5} Particulate Matter over the New York–New Jersey Harbor Estuary. *Atmos. Environ.* 36: 1077–1086.
- Hays, M.D., Cho, S.H., Baldauf, R., Schauer, J.J. and Shafer, M. (2011). Particle size distributions of metal and non-metal elements in an urban near-highway environment. *Atmos Environ.* 45(4): 925–34.
- Hering, S. and Cass, G. (1999). The magnitude of bias in measurement of PM_{2.5} arising from volatilization of particulate nitrate from Teflon filters. *Journal of the Air and Waste Management Association* 49: 725–733.
- Hueglin, C., Gehrig, R., Baltensperger, U., Gysel, M., Monn, C. and Vonmont, H. (2005). Chemical characterisation of PM_{2.5}, PM₁₀ and coarse particles at urban, near-city and rural

- sites in Switzerland. *Atmos. Environ.* 39: 637–651.
- Huo, M.Q., Sato, K., Ohizumi, T., Akimoto, H. and Takahashi, K. (2016). Characteristics of carbonaceous components in precipitation and atmospheric particle at Japanese sites. *Atmos. Environ.* 146:164-173.
- Husain, L. and Dutkiewicz, V.A. (1990). A long term (1975–1988) study of atmospheric SO_4^{2-} : regional contributions and concentration trends. *Atmos. Environ.* 24A: 1175–1187.
- Ikeda, K., Yamaji, K., Kanaya, Y., Taketani, F., Pan, X., Komazaki, Y., Kurokawa, J. and Ohara, T. (2014). Sensitivity analysis of source regions to $\text{PM}_{2.5}$ concentration at Fukue Island, Japan. *Journal of the Air & Waste Management Association* 64(4): 445–452.
- Ichikawa, Y., Neito, S., Ishii, K. and Oohashi, H. (2015). Seasonal Variation of $\text{PM}_{2.5}$ Components Observed in an Industrial Area of Chiba Prefecture, Japan. *Asian Journal of Atmospheric Environment* 9(1): 66-77.
- Iijima, A., Sato, K., Yano, K., Kato, M., Kozawa, K., Furuta, N. (2008). Emission factor for antimony in brake abrasion dusts as one of major atmospheric antimony sources. *Environmental Science and Technology.* 42(8): 2937–2942.
- Iijima, A., Sato, K., Fujitani, Y., Fujimori, E., Saito, Y., Tanabe, K., Ohara, T., Kozawa, K., Furuta, N. (2009). Clarification of the predominant emission sources of antimony in airborne particulate matter and estimation of their effects on the atmosphere in Japan. *Environmental Chemistry.* 6(2): 122–132.
- Inomata, Y., Ohizumi, T., Take, N., Sato, K. and Nishikawa, M. (2016). Transboundary transport of anthropogenic sulfur in $\text{PM}_{2.5}$ at a coastal site in the Sea of Japan as studied by sulfur isotopic ratio measurement. *Science of the Total Environment* 553: 617–625.
- JMA, <http://www.jma.go.jp/jma/index.html>, Last Access: 10 April 2017.
- Kaneyasu, N., Yamamoto, S., Sato, K., Takami, A., Hayashi, M., Hara, K., Kawamoto, K., Okuda, T. and Hatakeyama, S. (2014). Impact of long-range transport of aerosols on the $\text{PM}_{2.5}$ composition at a major metropolitan area in the northern Kyushu area of Japan. *Atmos.*

Environ. 97: 416-425.

Kennish, M.J. (1994). *Practical Handbook of Marine Science*, CRC Press, Boca Raton.

Khan, M. F., Shirasuna, Y., Hirano, K. and Masunaga, S. (2010). Characterization of PM_{2.5}, PM_{2.5-10} and PM_{>10} in ambient air, Yokohama, Japan. *Atmospheric Research* 96: 159–172.

Kikuchi, R., Sasaki, Y., Oba, A., Sato, A., Takada, M., Fujiwara, K., Kimoto, T., Ozeki, T., Sera, K. and Ogawa, N. (2010). Origin and Transportation Course of Heavy Metal Elements in the Particulate Matter (PM) at the Hachimantai Mountain Range in Northern Japan. *Soc. Mater. Eng. Resour. Japan* 17(2):177-181.

Kim, E., Hopke, P.K. and Edgerton, E.S. (2004). Improving Source Identification of Atlanta Aerosol Using Temperature Resolved Carbon Fractions in Positive Matrix Factorization. *Atmos. Environ.* 38: 3349–3362.

Kumagai, K., Iijima, A., Shimoda, M., Saitoh, Y., Kozawa, K., Hagino, H. and Sakamoto, K. (2010). Determination of Dicarboxylic Acids and Levoglucosan in Fine Particles in the Kanto Plain, Japan, for Source Apportionment of Organic Aerosols. *Aerosol Air Qual. Res.* 10: 282–291.

Leiva G, M. A., Santibañez, D.A., Ibarra E, S. and Matus C, P. (2013). A five-year study of particulate matter (PM_{2.5}) and cerebrovascular diseases. *Environmental Pollution* 181: 1–6.

Manousakas, M., Eleftheriadis, K. and Papaefthymiou, H. (2013). Characterization of PM₁₀ sources and ambient air concentration levels at Megalopolis City (Southern Greece) located in the vicinity of lignite-fired plants. *Aerosol and Air Quality Research* 13(3): 804–17.

Mason, B. (1966). *Principles of Geochemistry*, Wiley, New York.

MOEJ, <http://www.env.go.jp/air/osen/pm/html>, Last Access: 6 January 2016.

Murakami, Y. and Ono, M. (2006). Myocardial infarction deaths after high level exposure to particulate matter. *Journal of Epidemiology and Community Health* 60: 262–266.

Nakatsubo, R., Tsunetomo, D., Horie, Y., Hiraki, T., Saitoh, K., Yoda, Y. and Shima, M. (2014). Estimate of Regional and Broad-based Sources for PM_{2.5} Collected in an Industrial Area of

- Japan. *Asian Journal of Atmospheric Environment* 8-3:126-139.
- National Institute for Environmental Studies, <http://www.nies.go.jp/labo/crm-e/index.html>, Last Access: 12 October 2015.
- Network Center for EANET. (2010). *Technical Manual for Wet Deposition Monitoring in East Asia - 2010*, Asia Center for Air Pollution Research, Niigata.
- Network Center for EANET. (2016). *Report of the Inter-laboratory Comparison Project 2015*, Asia Center for Air Pollution Research, Niigata.
- Okuda, T., Tenmoku, M., Kato, J., Mori, J., Sato, T., Yokouchi, R. and Tanaka, S. (2006). Long-term Observation of Trace Metal Concentration in Aerosols at a Remote Island, Rishiri, Japan by Using Inductively Coupled Plasma Mass Spectrometry Equipped with Laser Ablation. *Water Air Soil Pollut.* 174: 3–17.
- Ouyang, W., Guo, B.B., Cai, G.Q., Li, Q., Han, S., Liu, B. and Liu, X.G. (2015). The washing effect of precipitation on particulate matter and the pollution dynamics of rainwater in downtown Beijing. *Science of the Total Environment* 505: 306–314.
- Pang, Y., Eatough, N.L. and Eatough, D.J. (2002). PM_{2.5} semivolatile organic material at riverside, California: implications for the PM_{2.5} Federal Reference Method sampler. *Aerosol Science and Technology* 36: 277–278.
- PMF 5.0, <https://www.epa.gov/air-research/epa-positive-matrix-factorization-50-fundamentals-and-user-guide>, Last Access: 12 May 2016.
- Reimann, C. and Caritat, P. (1998). *Chemical Elements in the Environment: Factsheets for the Geochemist and Environmental Scientist*, Springer, Berlin, Heidelberg.
- Sanchez-Romero, A., Sanchez-Lorenzo, A., Calbo, J., Gonzalez, J.A. and Azorin-Molina, C. (2014). The signal of aerosol induced changes in sunshine duration records: a review of the evidence. *J. Geophys. Res.* 119 (8): 4657–4673.
- Smichowski, P., Gómez, D.R., Frazzoli, C. and Caroli, S. (2008). Traffic-related elements in airborne particulate matter. *Appl. Spectros. Rev.* 43: 23-49.

- Shimada, K., Shimada, M., Takami, A., Hasegawa, S., Fushimi, A., Arakaki, T., Izumi, W. and Hatakeyama, S. (2015). Mode and Place of Origin of Carbonaceous Aerosols Transported From East Asia to Cape Hedo, Okinawa, Japan. *Aerosol Air Qual. Res.* 15: 799–813.
- Shimadera, H., Kondo, A., Kaga, A., Shrestha, K.L. and Inoue, Y. (2009). Contribution of transboundary air pollution to ionic concentrations in fog in the Kinki Region of Japan. *Atmos. Environ.* 43: 5894-5907.
- Speight, J.G. (2014). *The Chemistry and Technology of Petroleum*. CRC press, Boca Raton.
- Tang, N., Hattori, T., Taga, R., Igarashi, K., Yang, X.Y., Tamura, K., Kakimoto, H., Mishukov, V.F., Toriba, A., Kizu, R. and Hayakawa, K. (2015). Polycyclic aromatic hydrocarbons and nitropolycyclic aromatic hydrocarbons in urban air particulates and their relationship to emission sources in the Pan–Japan Sea countries. *Atmospheric Environment* 39(32), 5817–5826.
- Vladimir Alekseenko; Alexey Alekseenko. 2014. The abundances of chemical elements in urban soils. *Journal of Geochemical Exploration*. 147: 245–249.
- Wahlin, P., Berkowicz, R. and Palmgren, F. (2006). Characterisation of traffic-generated particulate matter in Copenhagen. *Atmos. Environ.* 40 (12): 2151–2159.
- Wang, Y.Q., Zhang, X.Y. and Draxler, R. (2009). TrajStat: GIS-based software that uses various trajectory statistical analysis methods to identify potential sources from long-term air pollution measurement data. *Environmental Modelling & Software* 24: 938-939.
- Yamazaki, S., Nitta, H., Ono, M., Green, J. and Fukuhara, S. (2007). Intracerebral haemorrhage associated with hourly concentration of ambient particulate matter: case-crossover analysis. *Occupational and Environmental Medicine* 64: 17–24.
- Yang, L.X., Wang, D.C., Cheng, S.H., Wang, Z., Zhou, Y., Zhou, X.H. and Wang, W.X. (2007). Influence of meteorological conditions and particulate matter on visual range impairment in Jinan, China. *Sci. Total Environ.* 383: 164–173.
- Yao, L., Yang, L.X., Yuan, Q., Yan, C., Dong, C., Meng, C.P., Sui, X., Yang, F., Lu, Y.L. And

- Wang, W.X. (2016). Sources apportionment of PM_{2.5} in a background site in the North China Plain. *Sci. Total Environ.* 541: 590-598.
- Ye, B., Ji, X., Yang, H., Yao, X., Chan, C.K., Cadle, S.H., Chan, T. and Mulawa, P.A. (2003). Concentration and chemical composition of PM_{2.5} in Shanghai for a 1-year period. *Atmos. Environ.* 37 (4): 499-510.
- Zang, H. S. (2015). Long-term variations in PM_{2.5} emission from open biomass burning in northeast Asia derived from satellite-derived data for 2000-2013. *Atmos. Environ.* 107: 342-350.
- Zeller, M., Giroud, M., Royer, C., Benatru, I., Besancenot, J.P., Rochette, L. and Cottin, Y. (2006). Air pollution and cardiovascular and cerebrovascular disease epidemiologic data. *Presse Med.* 35 (10): 1517–1522.
- Zhang, C., Ni, Z.W. and Ni, L.P. (2015). Multifractal detrended cross-correlation analysis between PM_{2.5} and meteorological factors. *Physica A* 438: 114 –123.